

AD

USAAML TECHNICAL REPORT 65-13

AN EXPERIMENTAL INVESTIGATION OF ROTOR HARMONIC AIRLOADS INCLUDING THE EFFECTS OF ROTOR-ROTOR INTERFERENCE AND BLADE FLEXIBILITY

By
Norman D. Ham
Paul A. Madden

May 1965

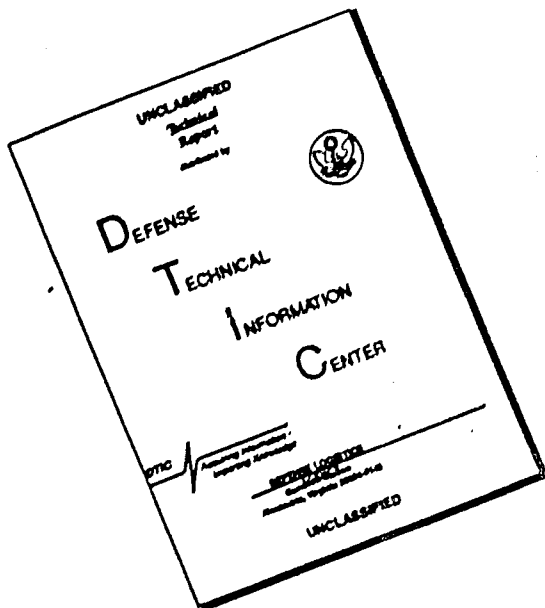
U. S. ARMY AVIATION MATERIEL LABORATORIES
FORT EUSTIS, VIRGINIA

CONTRACT DA 44-177-AMC-22(T)

MASSACHUSETTS INSTITUTE OF TECHNOLOGY



DISCLAIMER NOTICE



**THIS DOCUMENT IS BEST
QUALITY AVAILABLE. THE COPY
FURNISHED TO DTIC CONTAINED
A SIGNIFICANT NUMBER OF
PAGES WHICH DO NOT
REPRODUCE LEGIBLY.**

DDC Availability Notice

Qualified requesters may obtain copies of this report from DDC.

This report has been furnished to the Department of Commerce
for sale to the public.

Disclaimer

The findings in this report are not to be construed as an official
Department of the Army position, unless so designated by other
authorized documents.

When Government drawings, specifications, or other data are used
for any purpose other than in connection with a definitely re-
lated Government procurement operation, the United States Govern-
ment thereby incurs no responsibility nor any obligation what-
soever; and the fact that the Government may have formulated,
furnished, or in any way supplied the said drawings, specifica-
tions, or other data is not to be regarded by implication or
otherwise as in any manner licensing the holder or any person
or corporation, or conveying any rights or permission, to manu-
facture, use, or sell any patented invention that may in any way
be related thereto.

Disposition Instructions

Destroy this report when it is no longer needed. Do not return
to originator.

HEADQUARTERS
U S ARMY TRANSPORTATION RESEARCH COMMAND
FORT EUSTIS, VIRGINIA 23604

In this report, the Massachusetts Institute of Technology Aeroelastic and Structures Research Laboratory investigated harmonic spanwise airloads for single and tandem model rotor configurations at various rotor angles of attack, tip-speed ratios, and thrust loadings.

The experimental results are used in a discussion of rotor vibration levels at various harmonic airloads.

This Command has reviewed the report and considers it to be technically sound.

NOTE

On 1 March 1965, after this report had been prepared, the name of this command was changed from U.S. Army Transportation Research Command to:

U.S. ARMY AVIATION MATERIEL LABORATORIES

Task IP1215901A14203
Contract DA 44-177-AMC-22(T)
USAAML Technical Report 65-13

MAY 1965

AN EXPERIMENTAL INVESTIGATION OF
ROTOR HARMONIC AIRLOADS INCLUDING THE
EFFECTS OF ROTOR-ROTOR INTERFERENCE AND
BLADE FLEXIBILITY

by
Norman D. Ram
Paul A. Madden

Prepared by
Aeroelastic and Structures Research Laboratory
Massachusetts Institute of Technology
Cambridge, Massachusetts 02139

for
U. S. ARMY TRANSPORTATION RESEARCH COMMAND
FORT EUSTIS, VIRGINIA

SUMMARY

Experimental airload harmonics from the first to the tenth at various blade spanwise stations are presented for single and rear tandem rotor configurations for various rotor angles of attack, tip-speed ratios, and thrust loadings. The results include the effect of blade bending motion on airload harmonics for selected test cases.

Evaluation of the experimental results indicates several general conclusions of importance with regard to vibration levels of compound helicopters, tandem helicopters, and three- and four-bladed rotors.

PREFACE

This report was prepared by the Aeroelastic and Structures Research Laboratory of the Massachusetts Institute of Technology, Cambridge, Massachusetts, on U.S. Army Contract DA44-177-AMC-22(T). The project officers for the U.S. Army Transportation Research Command, Fort Eustis, Virginia were Mr. John E. Yeates and Lt. Francis E. LaCasse. The M.I.T. Project Supervisor was Professor Norman D. Ham, Department of Aeronautics and Astronautics; Mr. Paul A. Madden, Research Assistant, was responsible for data reduction and assisted in the test operations.

The contractor's report number is ASRL TR 117-1.

Grateful acknowledgement is made to Professor Rene H. Miller for his comments and suggestions, to Messrs. Oscar Wallin and Carl Fall of the Aeroelastic Model Shop for the construction of the models, to Mr. Fred Merlis, Research Engineer, ASRL, for the design of the electronic circuits, to the M.I.T. Computation Center, which made available the computer time necessary for the harmonic analysis of the test data, and to the Aerophysics Laboratory, M.I.T., for the loan of amplifiers.

CONTENTS

	<u>Page</u>
SUMMARY	iii
PREFACE	v
LIST OF ILLUSTRATIONS	viii
LIST OF SYMBOLS	ix
INTRODUCTION	1
CONCLUSIONS	2
EXPERIMENTAL PROGRAM	3
DISCUSSION OF EXPERIMENTAL RESULTS	8
REFERENCES	35
DISTRIBUTION	36
APPENDICES	
I Rotor Characteristics	37
II Test Conditions	38
III Test Results	40

ILLUSTRATIONS

<u>Figure</u>		<u>Page</u>
1	Rotor Test Rig	11
2	Pressure Calibration Equipment	12
3	Test Section Velocity Profiles	13
4	Circuit Schematic	14
5	Recording System	15
6(a)-(f)	Nondimensional Third Harmonic Airload Amplitudes for the Single Rotor with Rigid Blades	16
7(a)-(c)	Nondimensional Third Harmonic Airload Amplitudes for the Rear Tandem Rotor with Rigid Blades	22
8(a)-(c)	Nondimensional Sixth Harmonic Air- load Amplitudes for the Rear Tandem Rotor with Rigid Blades	25
9(a)-(c)	Nondimensional Third Harmonic Airload Amplitude Comparison -- Three- and Four-Bladed Rotors	28
10(a)-(c)	Nondimensional Fourth Harmonic Airload Amplitude Comparison -- Three- and Four-Bladed Rotors	29
11	Nondimensional Third Harmonic Airload Amplitudes for the Single Rotor with Flexible Blades in Bending Resonance	34

SYMBOLS

$ l_n $	nondimensional magnitude of harmonic airload, $ L_n $, fraction of L_o/R
n	harmonic number
x	nondimensional blade spanwise station, fraction of rotor radius
C_T	rotor thrust coefficient, thrust divided by air density, disk area, tip speed squared
L_o	steady-state thrust of one blade, pounds
L_n	harmonic airload acting at one blade station, pounds per inch, $L_n = L_{n_c} \cos n\psi + L_{n_s} \sin n\psi$
L_{n_c}	cosine component of harmonic airload acting at one blade station, pounds per inch
L_{n_s}	sine component of harmonic airload acting at one blade station, pounds per inch
R	rotor radius, feet or inches
α	rotor shaft angle, positive aft of vertical, degrees. Since rotor has no cyclic pitch, also no feathering axis angle, degrees
μ	rotor advance ratio, free-stream velocity divided by rotor tip speed
ψ	blade azimuth angle, zero when instrumented blade downstream, degrees
σ	rotor solidity, blade area divided by disk area
SR	single rotor configuration
TRR	rear rotor of tandem configuration
(R)	articulated blade, relatively rigid in bending
(F)	articulated blade, relatively flexible in bending

Subscripts

f front rotor

r rear rotor

nom nominal value for purposes of classification

INTRODUCTION

Rotor-induced vibration is a problem of major significance in current helicopter technology. The difficulty of designing for minimum vibration levels is largely due to the lack of knowledge of the harmonic airloads acting on the rotor blades themselves. Considerable extremely valuable flight test data have become available for two- and four-bladed rotors. However, in such flight tests, the necessity of keeping the aircraft in trim prevents a wide variation of such major parameters as rotor angle of attack and blade loading, while manufacturing costs prohibit major changes in such parameters as rotor blade flexibility and tandem rotor geometry. Also, very large vibratory loads occur at transition flight speeds that are difficult to achieve in steady free flight. Yet, extensive data at these speeds are urgently required due to the occurrence of extreme wake distortion which greatly contributes to the large magnitude of the harmonic airloads and increases the difficulty of theoretical prediction of these harmonic airloads. (See References 1, 2, 3, and 4).

The purpose of the present study is to present and assess extensive harmonic airload data obtained in the wind tunnel for simulated transition flight with three-bladed rotors in both single and tandem configurations for wide variations in rotor angle of attack, blade loading, and blade flexibility.

This study is a continuation of a number of investigations that have been conducted over the past several years on rotor vibration and airload problems. The equipment developed during these past investigations was utilized during the current study.

CONCLUSIONS

The rotor orientations and blade loadings associated with a compound helicopter having auxiliary propulsion units and lifting surfaces lead to harmonic airload amplitudes comparable with those of pure helicopters at moderate forward speeds.

The orientation of the rear rotor of a tandem helicopter relative to the front rotor is of fundamental importance in establishing rear rotor harmonic airload amplitudes, particularly during transition.

There is no significant difference between the dominant harmonic airload amplitudes of three- and four-bladed single rotors operating under identical flight conditions.

EXPERIMENTAL PROGRAM

Test Stand

The test stand consists of two pylons mounted on heavy steel beams in such a way that the front pylon can be moved fore and aft to vary the rotor overlap. Both the front and rear pylon can be raised to vary the rotor stagger (Figure 1). For the present tests the rotors were at the same height and overlapped 67 percent of the rotor radius.

The pylons are made of welded steel channels, and provision has been incorporated to tilt the rotor heads from 5° aft to 15° forward by remote control of an electric-motor-driven linkage. The rotor power is supplied by a 10-horsepower hydraulic motor, controlled from outside the tunnel. Two right-angle gearboxes and a connecting shaft with constant velocity joints turn the front rotor shaft synchronously with the rear shaft, but in the opposite direction.

In the single rotor configuration, the front rotor pylon and the connecting shaft are removed.

Appendix I lists the principal parameters of the rotors.

Rotors

Both front and rear rotors are 8 feet in diameter and have three fully articulated (flapping and lagging degrees of freedom) blades with no mechanical dampers and no cyclic pitch control. The blades are rigid in torsion.

Thirty-three slip rings are available to transmit pressure signals from the rotating hub to the amplifiers and recording equipment. Three spring strip brushes wired in parallel bear on each slip ring. A timing signal is generated every time the instrumented blade passes through azimuth angle 90°.

The flapping displacement of the blade is measured by means of a spring steel beam between the flapping pin and the hub, with two active arm strain gage bridges mounted on the beam. The angular displacement signal is linear over the whole range of measurement. The dummy arms of the strain gage bridges consist of precision resistors mounted on the top surface of the hub, so that the bridges are complete on the rotor side of the slip rings.

Pressure Measurements

Variable reluctance transducers (Reference 7) with a differential pressure range of 0 to 2 psi are installed in the instrumented blade against the front face of the spar, oriented so that readings are not affected by centrifugal force or blade flapping accelerations, and connected by .040-inch-diameter hypodermic tubing to the pressure tap locations on the upper and lower surfaces of the blade. Eight such locations were chosen, all at the 10 percent chordwise station and at the 20 percent, 40 percent, 60 percent, 70 percent, 80 percent, 85 percent, 90 percent, and 95 percent spanwise stations.

Each transducer was calibrated statically and dynamically before installation in the blade (Figure 2). Static calibrations of all pressure transducers were performed frequently during test operations. The transducers had a flat response to sinusoidal pressure oscillations at frequencies from 0 to 70 cycles per second but were not tested beyond this frequency, which corresponds to the tenth harmonic of the rotor at 400 rpm.

Model Blades

All blades are of 0012 cross section with uniform chord mass and stiffness and incorporate 10° of linear twist. The rigid blades consist of a partially flattened 2024-T3 aluminum-tube spar with a hardwood leading edge and a balsa-covered, ribbed, trailing edge. The flexible blades employ a solid rectangular section aluminum spar with solid chordwise-grain-balsa leading- and trailing-edge portions. The pressure transducers are attached to the leading edge of the spar of one instrumented blade, and corresponding lead ballast is added to the other blades. The elastic axis and the c.g. are at the quarter chord. Lead tape was applied at the trailing edge to attain the desired c.g. location.

Two strain gages were mounted on the spar of one of the flexible blades at 30 percent of the span to provide a bending signal that was displayed on the oscilloscope to indicate the onset of blade bending resonance.

The blade root attachment fittings include a worm and gear mechanism to permit adjustment of the collective pitch as well as to facilitate tracking of the blades.

Wind Tunnel

All tests were conducted in the 9-foot by 12-foot return test section of the Aeroelastic and Structures Research Laboratory Flutter Tunnel at MIT. To provide a uniform velocity distribution over the test section and to minimize the turbulence and swirl created by the upstream fan, the test section was modified as follows: New walls were built to eliminate tunnel expansion at the test section; a vertical mid-divider from floor to ceiling was placed from the tunnel fan downstream to an existing vertical beam to cut the one large swirl into two smaller swirls and to bring additional velocity into the center section; a trailing edge fairing was placed on the beam to smooth the flow; two coarse damping screens made of stretched steel sheets were placed at the end of the divider to create a back pressure and to even the flow, and a fine mesh damping screen was placed downstream of the coarse screens to minimize turbulence from both the fans and the coarse screens. Velocity profiles across the test section are presented in Figure 3.

The effect of tunnel turbulence on the higher harmonic airloads was not investigated quantitatively. However, the repeatability of the blade pressure test records indicated the effect to be negligible for tip-speed ratios of .05 and .10. At a tip-speed ratio of .20, the increased turbulence due to the higher tunnel speed caused significant random changes in amplitude and phase of pressure harmonics above the sixth order of rotor rotational speed. However, these harmonics were of such small magnitude that it was not considered worthwhile to perform a statistical analysis of many test cycles to eliminate the random effect of turbulence.

No corrections were applied to the data to account for the effects of tunnel wall interference. Although such corrections would affect the magnitude of the steady-state airload by five percent or less, it is expected that they would not significantly influence the higher harmonic airloads.

Test Procedure

Tests were run on both tandem and single rotors at various blade loadings, rotor angles of attack, and tip-speed ratios (see Appendix II). A stroboscope was used to monitor rotor rotational speed and blade tracking.

All blades were tracked to the instrumented blade tip at the pitch settings and rotor speed for the given test condition.

Instrumentation

The strain gage bridges were excited with 5-volt DC and the pressure transducers with a 20-kc, 5-volt carrier system.

Because of the number of channels involved, it was found necessary to use two separate four-channel carrier amplifiers, with synchronized excitations. The flapping signal did not require amplification.

All the channels were recorded simultaneously on an oscillograph using galvanometers having a natural frequency of 400 cycles per second. The complete recording system is shown in Figures 4 and 5.

Data Reduction and Accuracy

One typical cycle of each pressure channel trace for a given test condition was subjected to a 40- to 48-point harmonic analysis that yielded all harmonics up to the tenth. In the course of the analysis, calibration factors were applied to convert inches of pressure trace deflection to pressure in pounds per square inch. A conversion factor of 2.175 was also applied to convert these pressure readings (at 10-percent chord) to the equivalent total loading in pounds per inch at that spanwise station, following the method described in Reference 8. This technique is valid for the moderate blade mean lift coefficient (0.6) and the low advancing blade tip Mach number (0.15) of the present tests.

Due to the low ratio of the highest airload frequency of interest (67 cycles per second or tenth harmonic) to the galvanometer natural frequency (400 cycles per second), the maximum error in amplitude response of the galvanometer (for 64-percent damping ratio) was less than 1 percent. Similarly, for the above damping ratio, the phase angle error corresponds to a blade azimuth lag angle of about 1.5° for all airload harmonics. Both these errors were considered negligible. The phase lag is constant due to the linear variation of phase angle with frequency ratio for a second-order dynamic system with 64-percent damping ratio.

The pressure gage itself has a natural frequency (including inlet tubing) of greater than 2000 cycles per second and a damping ratio of the order of 0.1 (Reference 7); hence, errors due to its dynamic response to frequencies of 67 cycles per second or less will be negligible. Errors due to gage hysteresis are less than 1 percent of maximum pressure experienced (References 7 and 9).

From the above considerations, errors in the measured harmonic airload data can be expected to be less than 5 percent of the measured values.

Data Presentation

Test conditions are specified in Appendix II. Included for convenience is the steady-state lift acting on one blade at each test condition.

Test results are presented in Appendix III in terms of airload harmonics up to the tenth at various spanwise stations. Steady-state data are also presented, though due to instrumentation drift, much of these data had to be corrected by interpolation and are approximate only. They are believed to be within 10 percent of the actual value.

DISCUSSION OF EXPERIMENTAL RESULTS

Detailed experimental results are presented in Appendix III. In order to evaluate the effect of variation of rotor parameters upon helicopter vertical vibration levels, certain harmonic airload amplitudes were expressed as a ratio of the mean blade airload- L_o/R and plotted against spanwise station, for various shaft angles, tip-speed ratios, and blade loadings. Note that the values of C_T/c shown are nominal only. Actual values for individual test points can be obtained using the values of L_o given in Appendix II. Since, for a given test condition, these amplitudes have different phasings for different spanwise stations, such values do not represent an actual spanwise loading at a given instant of time. However, it is a useful qualitative indication of the harmonic excitation acting on a rotor blade in a given test condition.

Significant airload harmonics for vertical vibration of a three-bladed rotor are the third, sixth, and ninth. Nondimensional third-harmonic amplitudes for a single rotor with rigid blades are shown in Figure 6. Here, the term "rigid" implies that the blade first mode bending frequency was far higher than third harmonic (see Appendix I). Sixth and ninth harmonic amplitudes for this rotor configuration were found in general to be much smaller than the third harmonic (see Appendix III).

Two general characteristics of the higher harmonic airloads are evident in Figure 6: the concentration near the tip, and the rapid spanwise fluctuations. These characteristics necessitate a corresponding concentration of airload transducers near the tip when such airloads are measured.

The well-known increase in harmonic excitation as the rotor angle of attack is increased at very low flight speeds (e.g., during flares) is indicated by Figure 6. This effect is due to the corresponding decrease in rotor inflow that permits the blade tip vortices to remain close to the rotor. The figure indicates that this effect also occurs at moderate flight speeds ($\alpha = .20$), though the increase here tends to occur at inboard stations. This point may be of significance for helicopters with auxiliary propulsion, since such helicopters operate with low rotor inflows.

The variation of harmonic airloads with blade loading- C_T/c is seen to be most pronounced at moderate flight speeds (Figures 6(c) and (f)). At lower flight speeds, the reduced inflow, and consequent close proximity of the trailing vortices to the rotor, is apparently somewhat offset by the reduced strength of the vortices. The effect of reduction of blade loading is

most pronounced at moderate flight speeds, since changes in mean downwash, and, hence, vortex spacing, are now directly related to changes in thrust ($\lambda \sim C_T$ rather than $\sim \sqrt{C_T}$).

The detrimental effect of reducing C_T/σ will be of concern in the design of compound helicopters utilizing auxiliary wings to unload the rotor in cruising flight.

The familiar reduction in harmonic airloads with forward speed is illustrated by Figure 6. This reduction is, of course, due to the increase in the rate of passage of rotor vorticity downstream.

Third and sixth harmonic airloads for the rear rotor of a tandem configuration with rigid blades are shown in Figures 7 and 8. The sixth harmonic airloads are included, since they are of a magnitude comparable to the third harmonic for the tandem rotor. It should be noted that in certain cases significant ninth harmonic airloads occur on the rear tandem rotor and that in many cases other higher harmonic airloads are of appreciable magnitude for this configuration (see Appendix III), apparently due to the proximity of the trailing vorticity from the front rotor. However, detailed discussion of these harmonics is not presented here.

Figure 7 shows that the third harmonic excitation of the rear tandem rotor is comparable to that of the single rotor, Figure 6. Note that the tandem airloads tend to be more distributed over the blade span, with appreciable amplitudes at the inboard stations.

The figures also illustrate the complex variation of harmonic airloads with changes in rear rotor orientation with respect to the front rotor. It would appear to be advantageous to trim the rear rotor to a position as far from the front rotor trailing vorticity as possible for minimum rear rotor outboard harmonic excitation. However, the inboard harmonic airload is increased. This paradox is apparently due to the outboard harmonic airloads being largely due to vorticity trailed from the front rotor; hence, rearward tilt moves the rear rotor away from this vorticity, while on the other hand, the trailing vorticity of the rear rotor now remains close to that rotor and increases the inboard harmonic airload as in the case of the single rotor.

Shaft angles for the tandem rotor configuration of this investigation that lead to rotor trim positions typical for a full-scale aircraft in free flight are as follows:

$\frac{u}{}$	$\frac{\alpha_F}{}$	$\frac{\alpha_R}{}$
.05	-5°	0°
.10	-5°	0°
.20	-10°	0°

The value for $u = .10$ provides insufficient rotor angular separation for minimum harmonic excitation according to the present results. However, α_F can be readily decreased (rotor tilted forward) in an accelerating transition and α_R can be increased (rotor tilted aft) in a decelerating transition.

Third and fourth harmonic wind tunnel airloads for the three-bladed model rotor of the present study are compared with those for the four-bladed full scale free flight rotor of Reference 2 in Figures 9 and 10 for similar test conditions. Of interest are the similar character and magnitude of identical harmonics even for such wide variations in test environment and rotor configuration. The data also indicate that there is no significant difference in the predominant harmonic excitation (third harmonic for three-bladed rotors, fourth harmonic for four-bladed rotors) for rotors with three and four blades. This result is apparently due to the fact that though the trailing vortices of a four-bladed rotor are closer to the blades than they would be for a three-bladed rotor producing the same thrust under the same flight condition, the strength of the individual vortices is also reduced and the two effects approximately cancel in terms of airloads induced on the blades. Note that M.I.T. flexible blade results (Case 43) are almost identical to the results of Reference 2.

The third harmonic airload measured on the flexible blade in bending resonance with the third harmonic airload is shown in Figure 11 for comparison with the results shown in Figure 6(e) for the rigid blade far from third harmonic resonance.

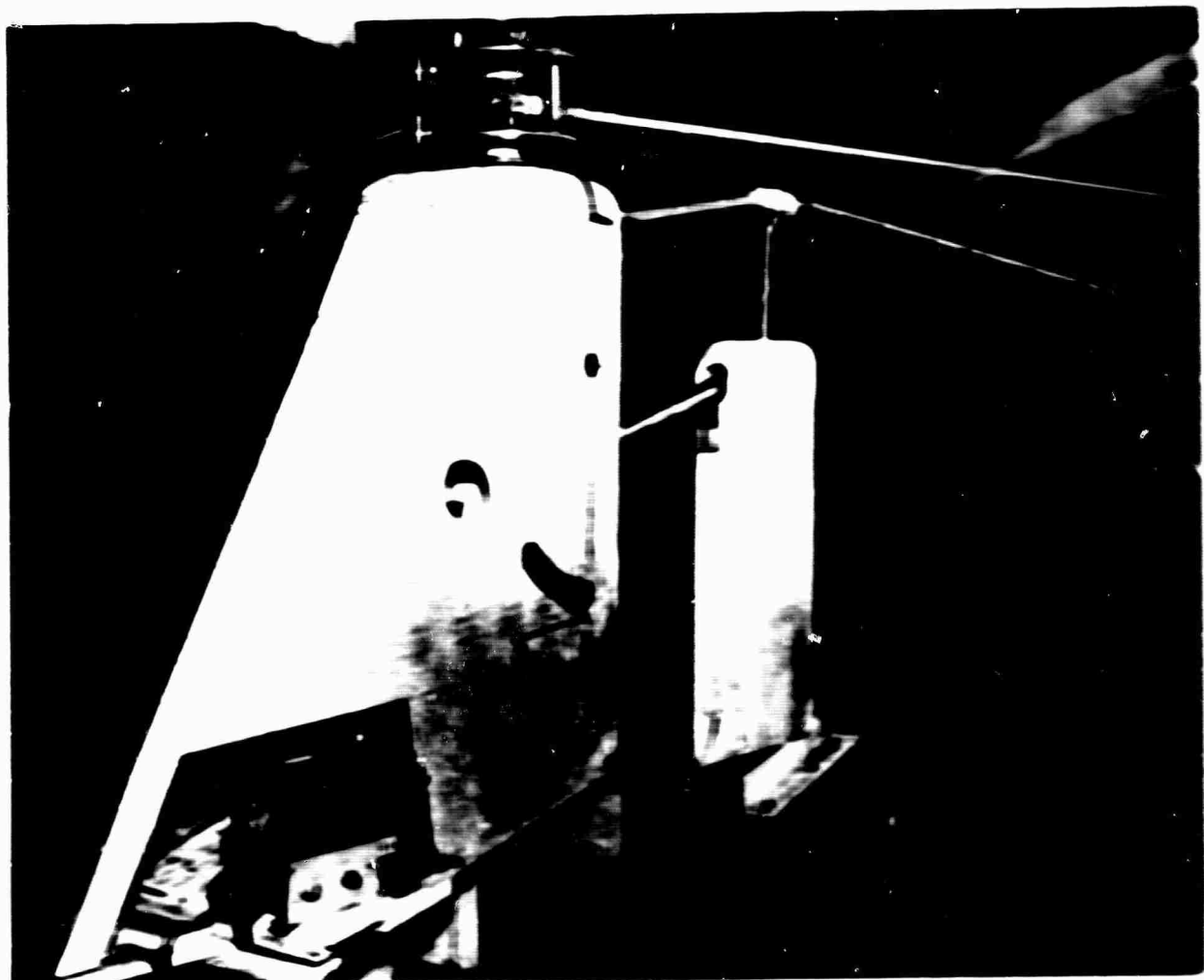


FIGURE 4. MOTOR TEST RIG

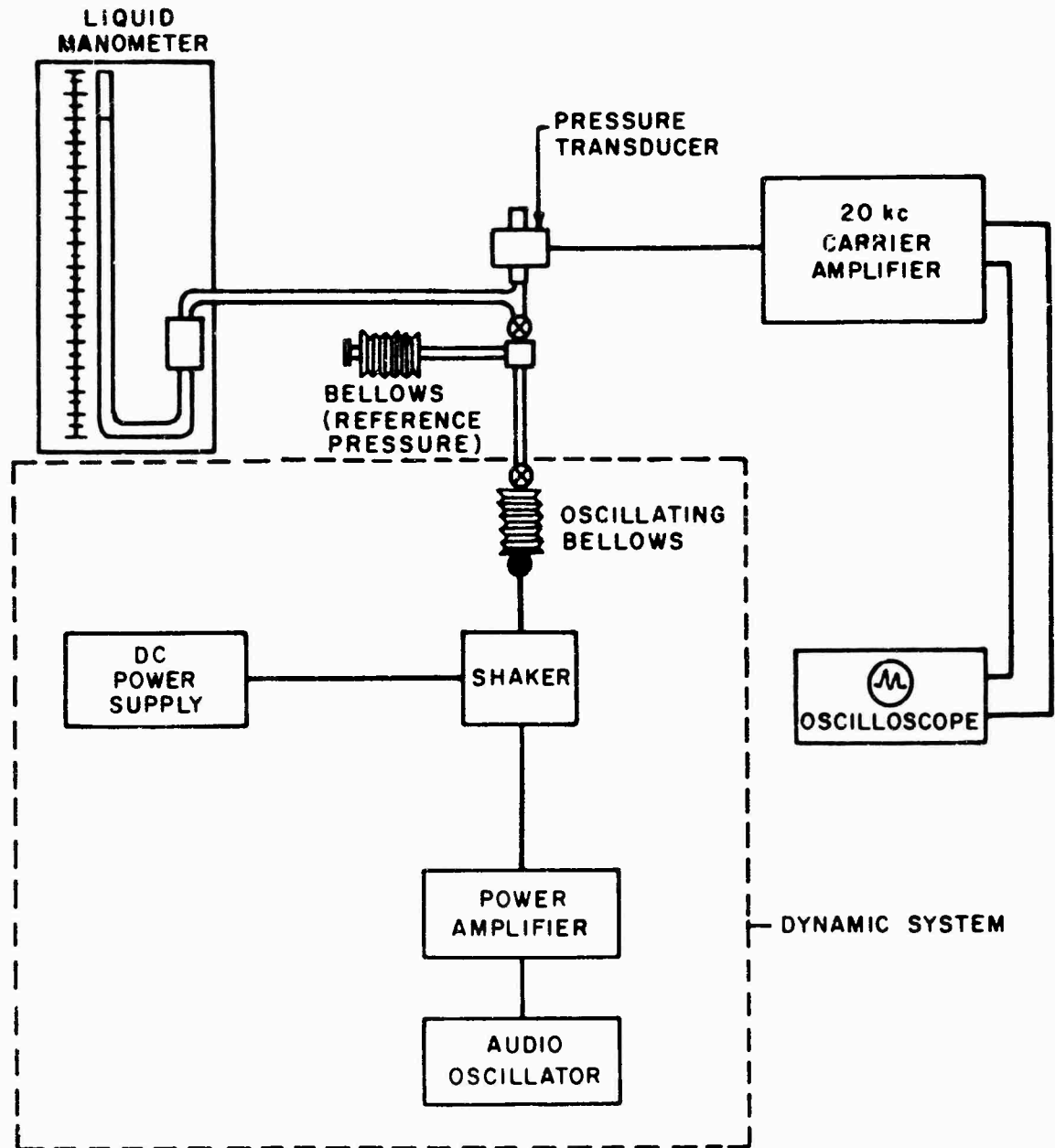


FIGURE 2. PRESSURE CALIBRATION EQUIPMENT.

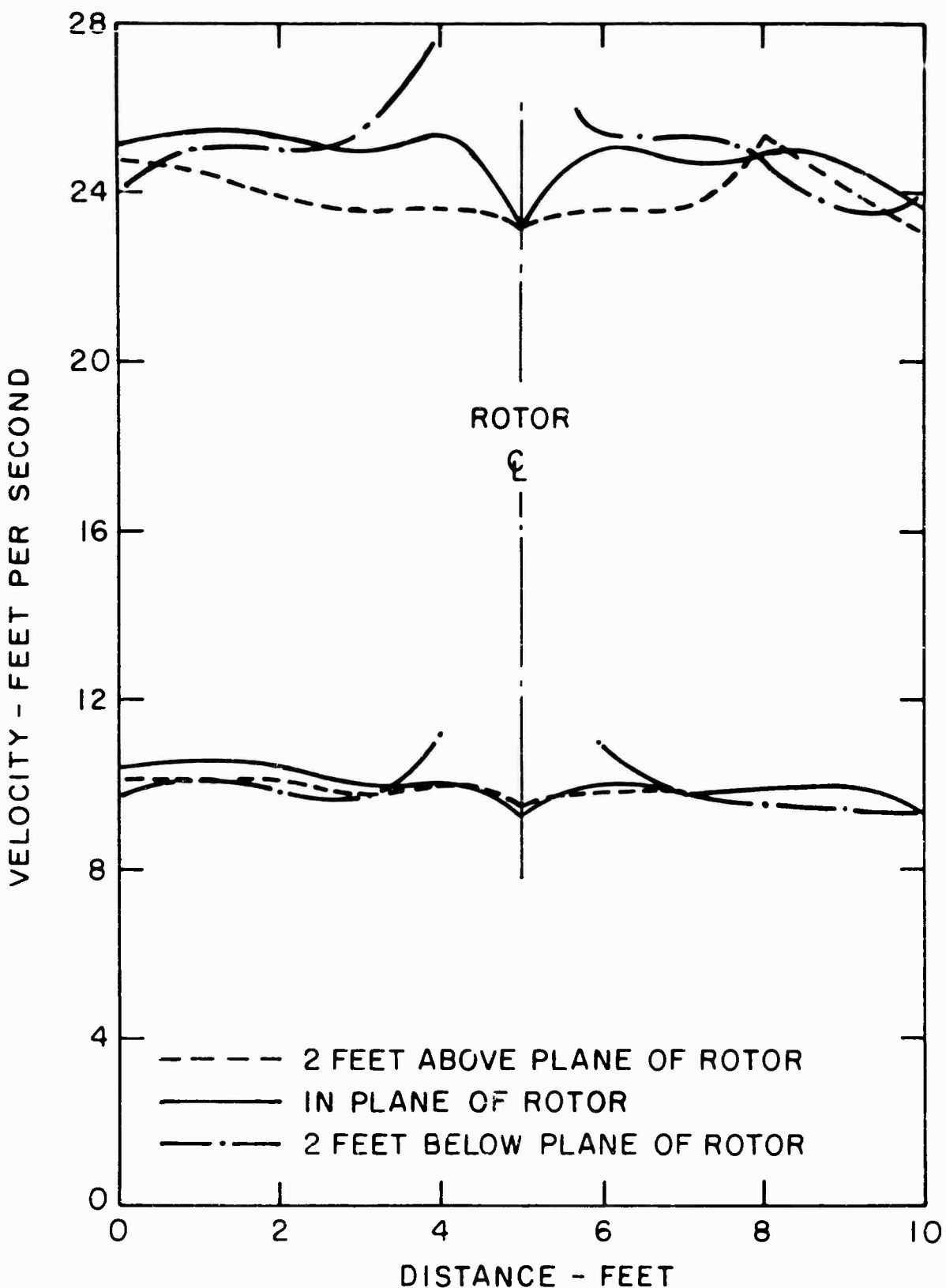
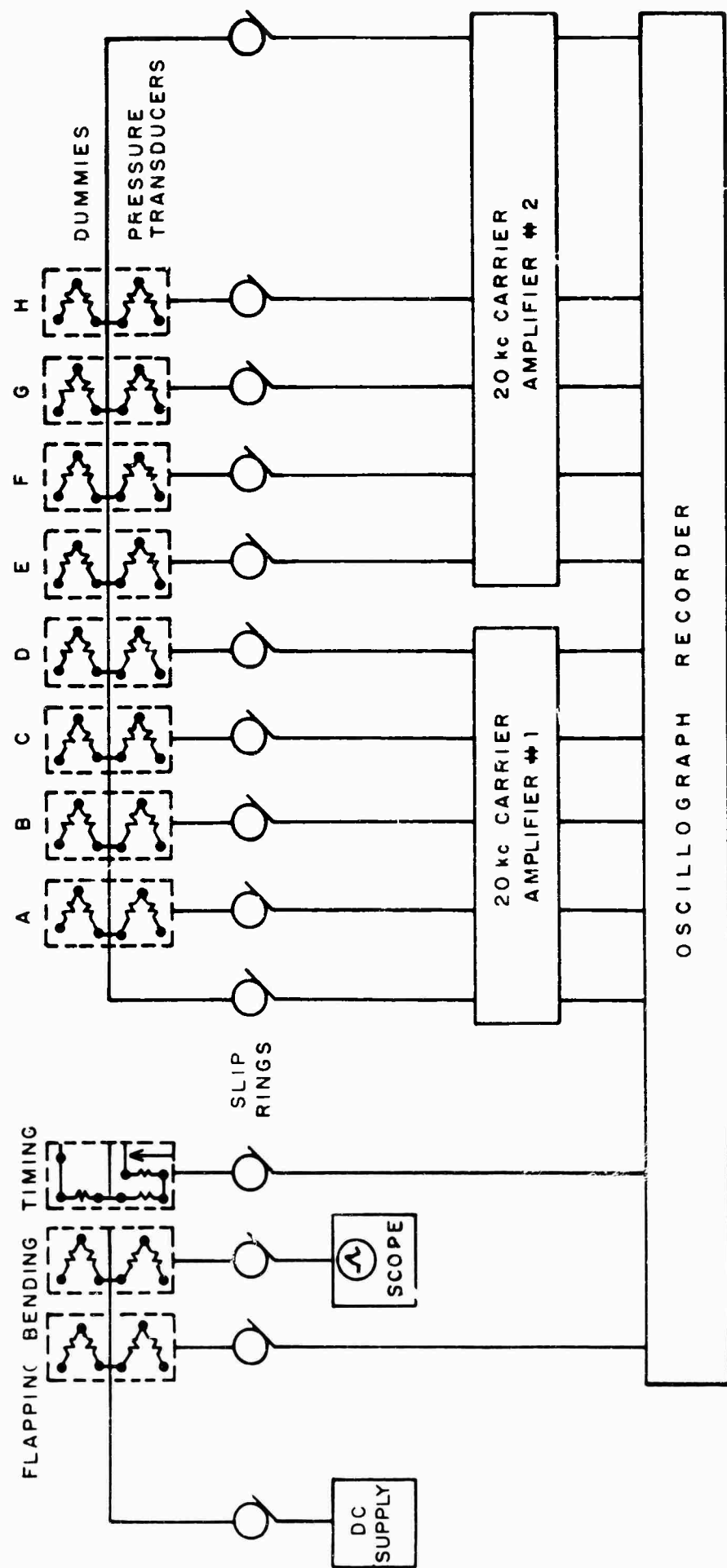


FIGURE 3. TEST SECTION VELOCITY PROFILES.

FIGURE 4. CIRCUIT SCHEMATIC.



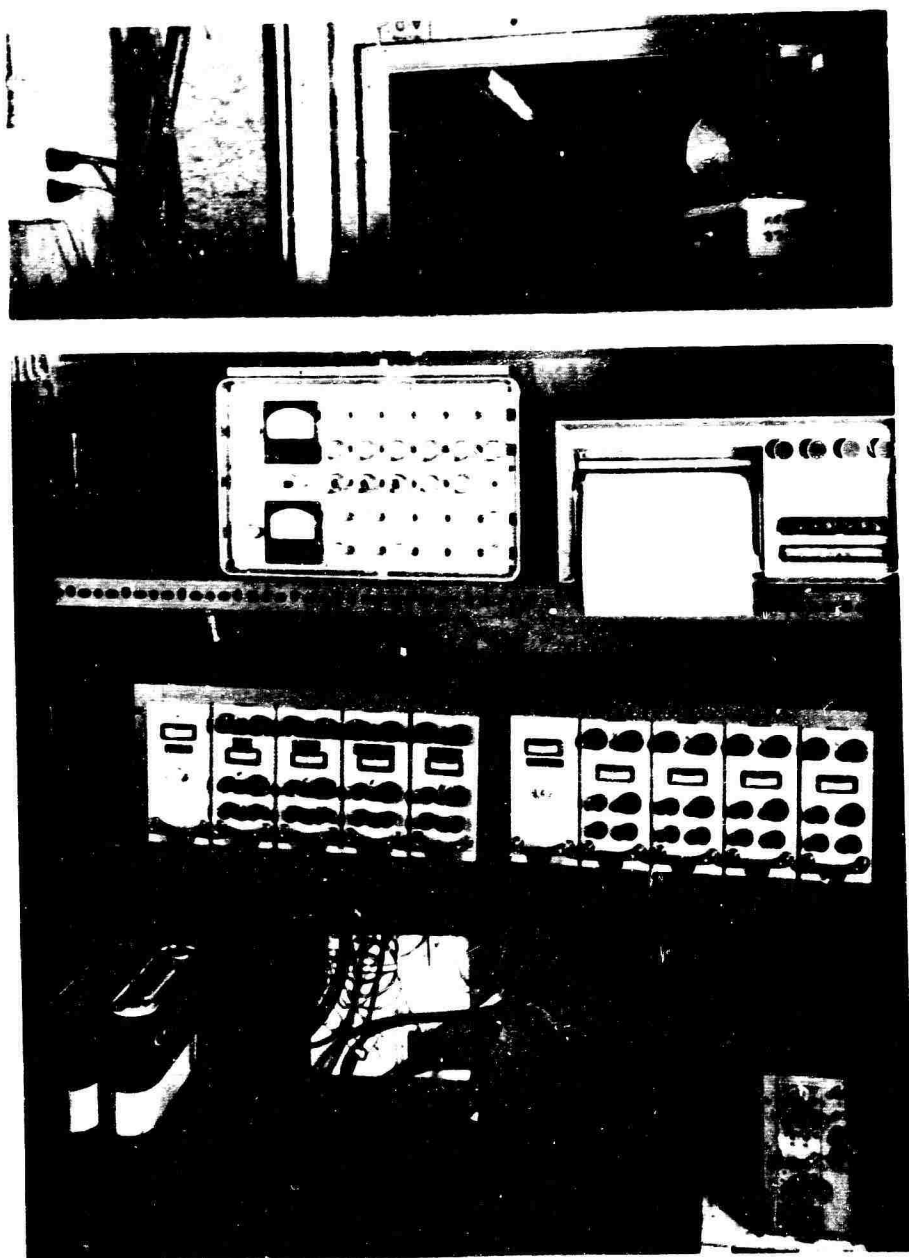


FIGURE 5. RECORDING SYSTEM.

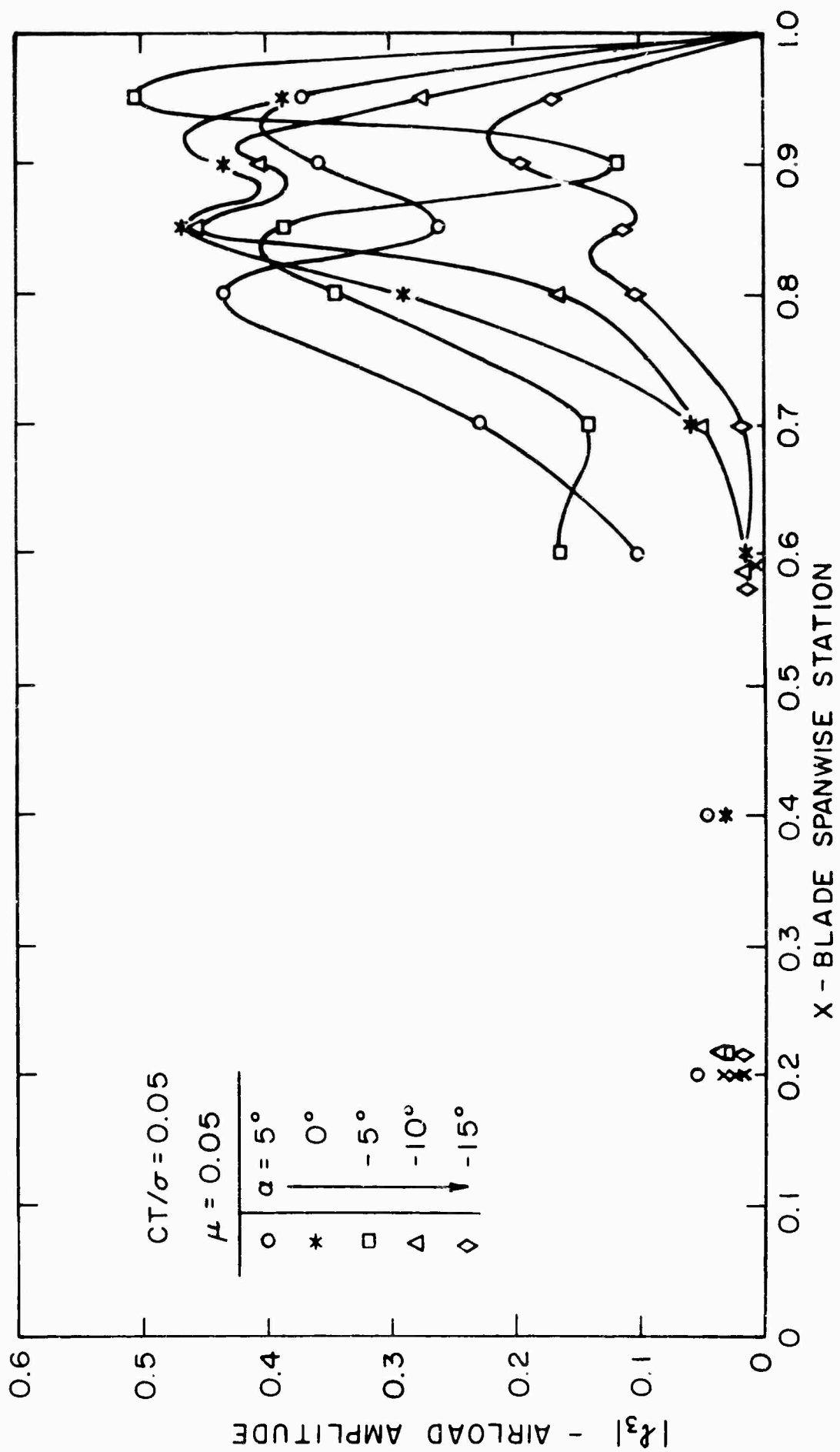


FIGURE 6(a) NONDIMENSIONAL THIRD HARMONIC AIRLOAD AMPLITUDES FOR THE SINGLE ROTOR WITH RIGID BLADES.

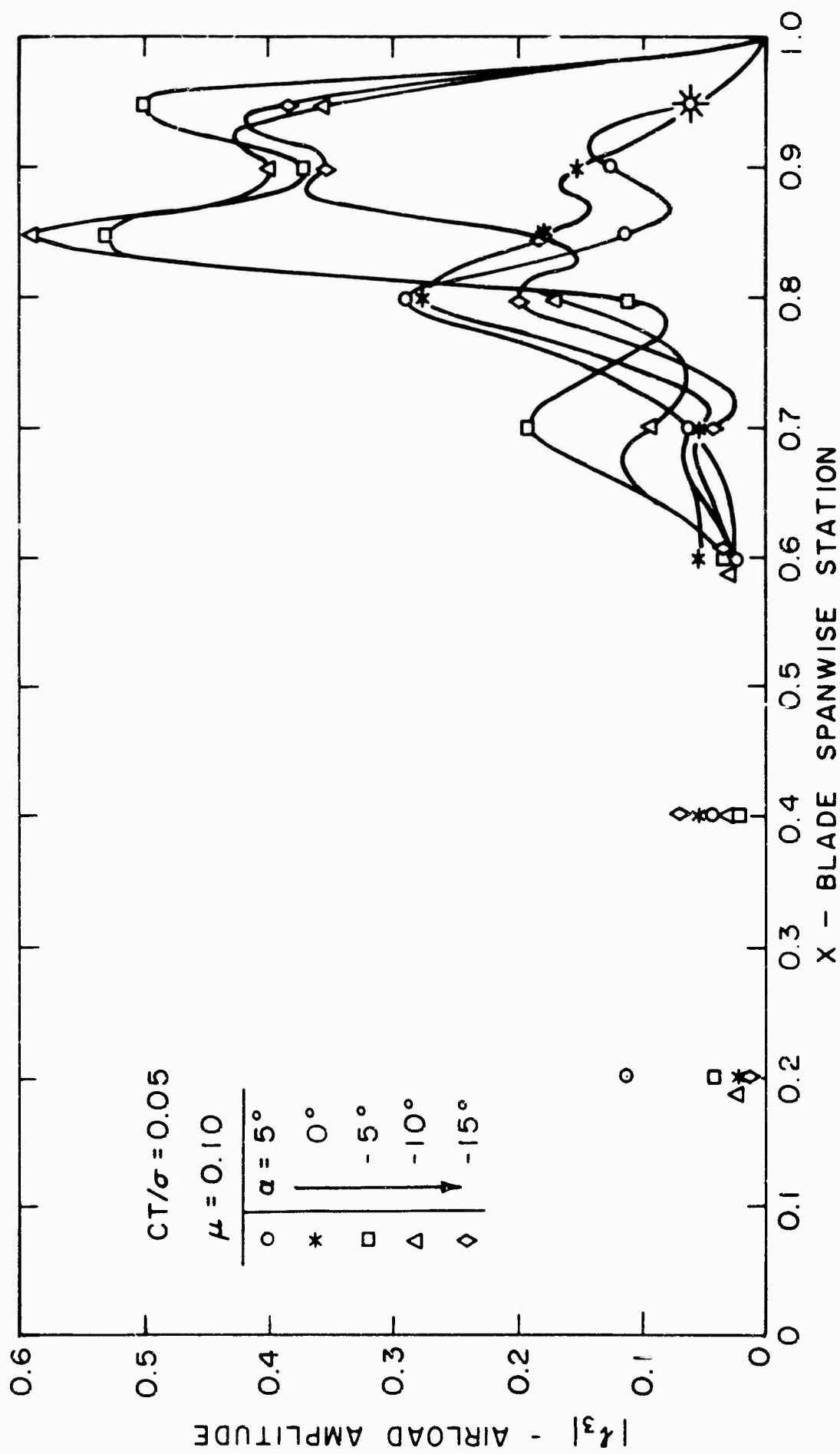


FIGURE 6 (b).

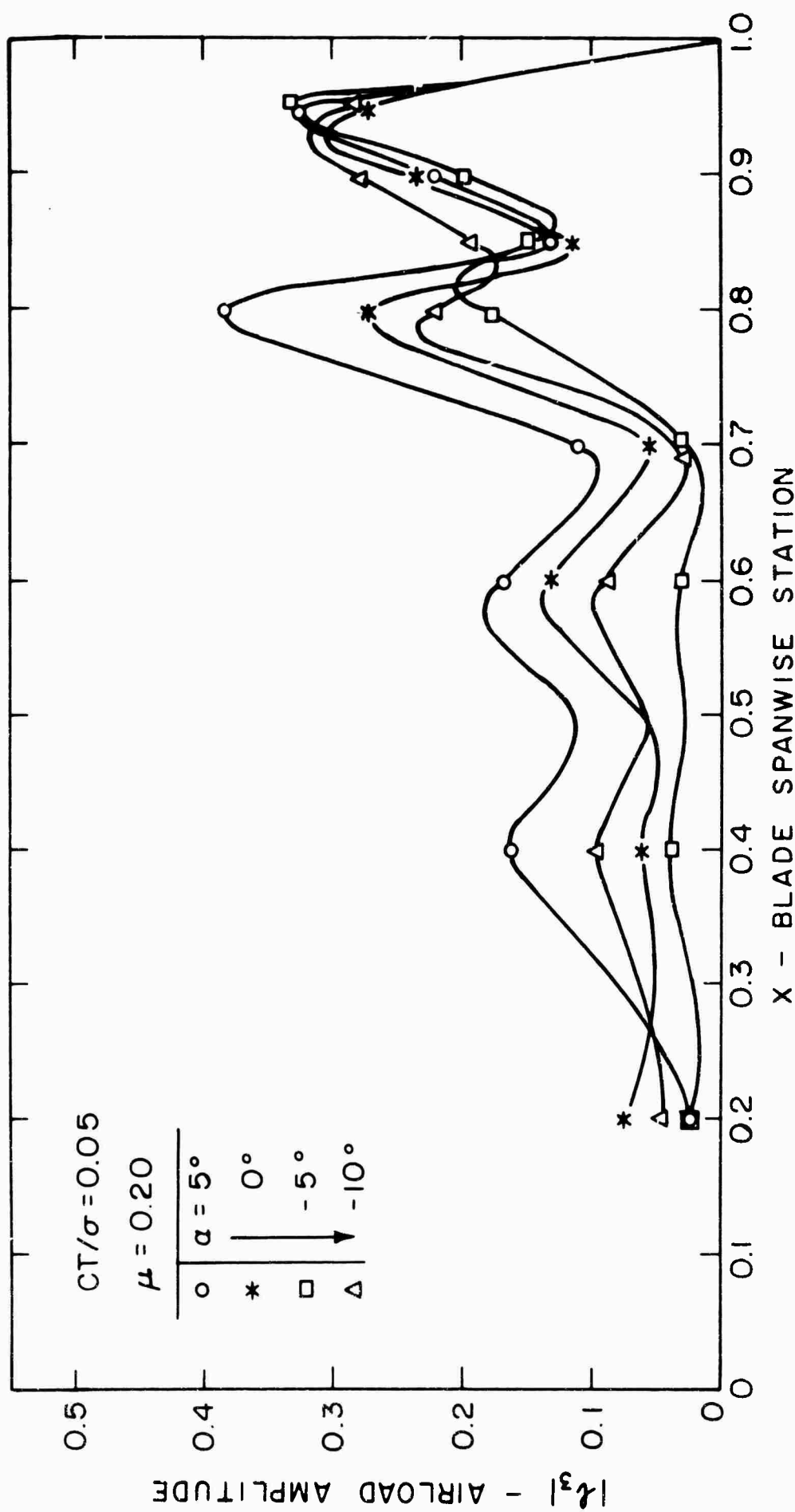


FIGURE 6 (c).

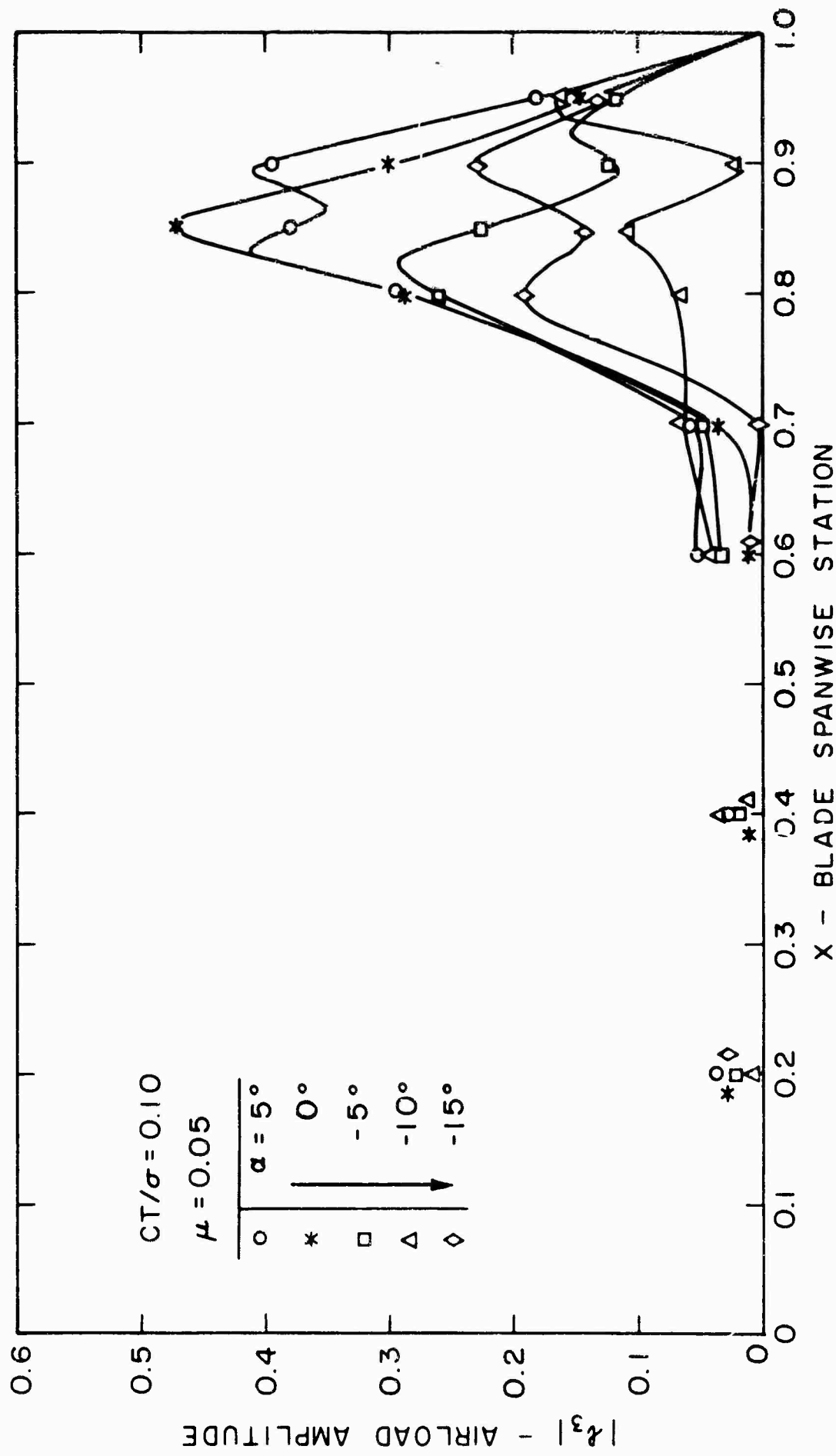
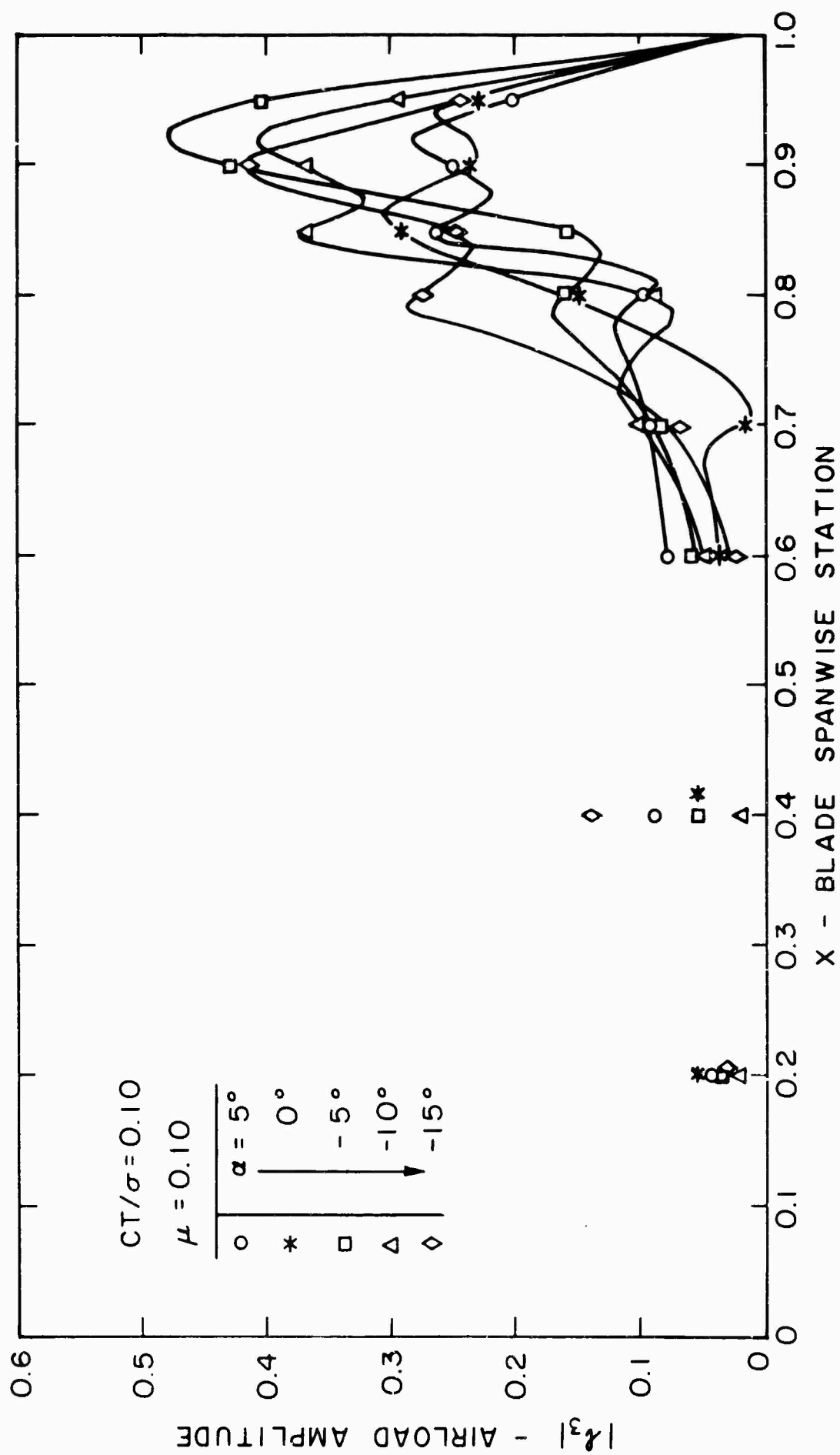


FIGURE 6(d).

FIGURE 6(e).



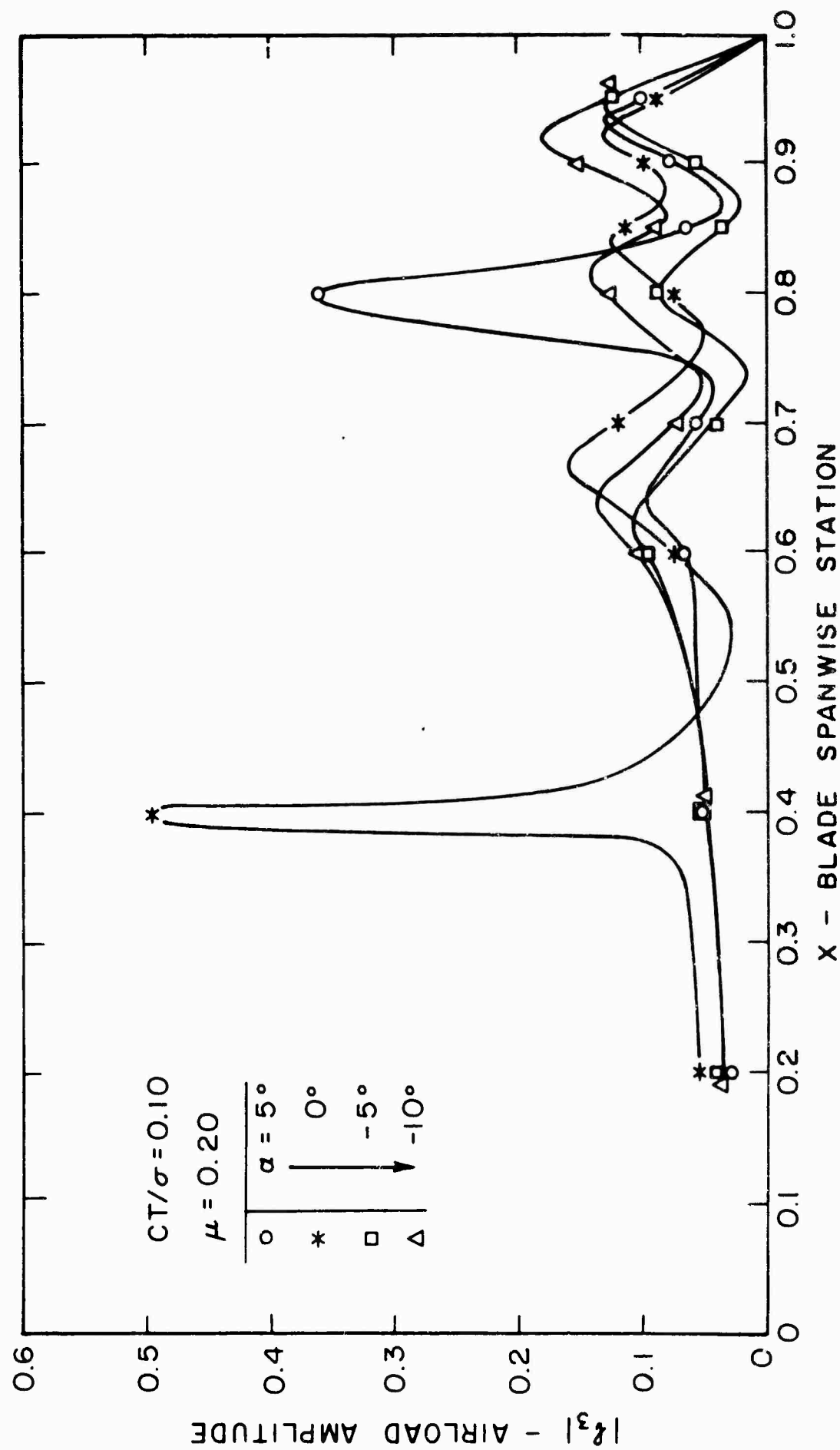


FIGURE 6(f).

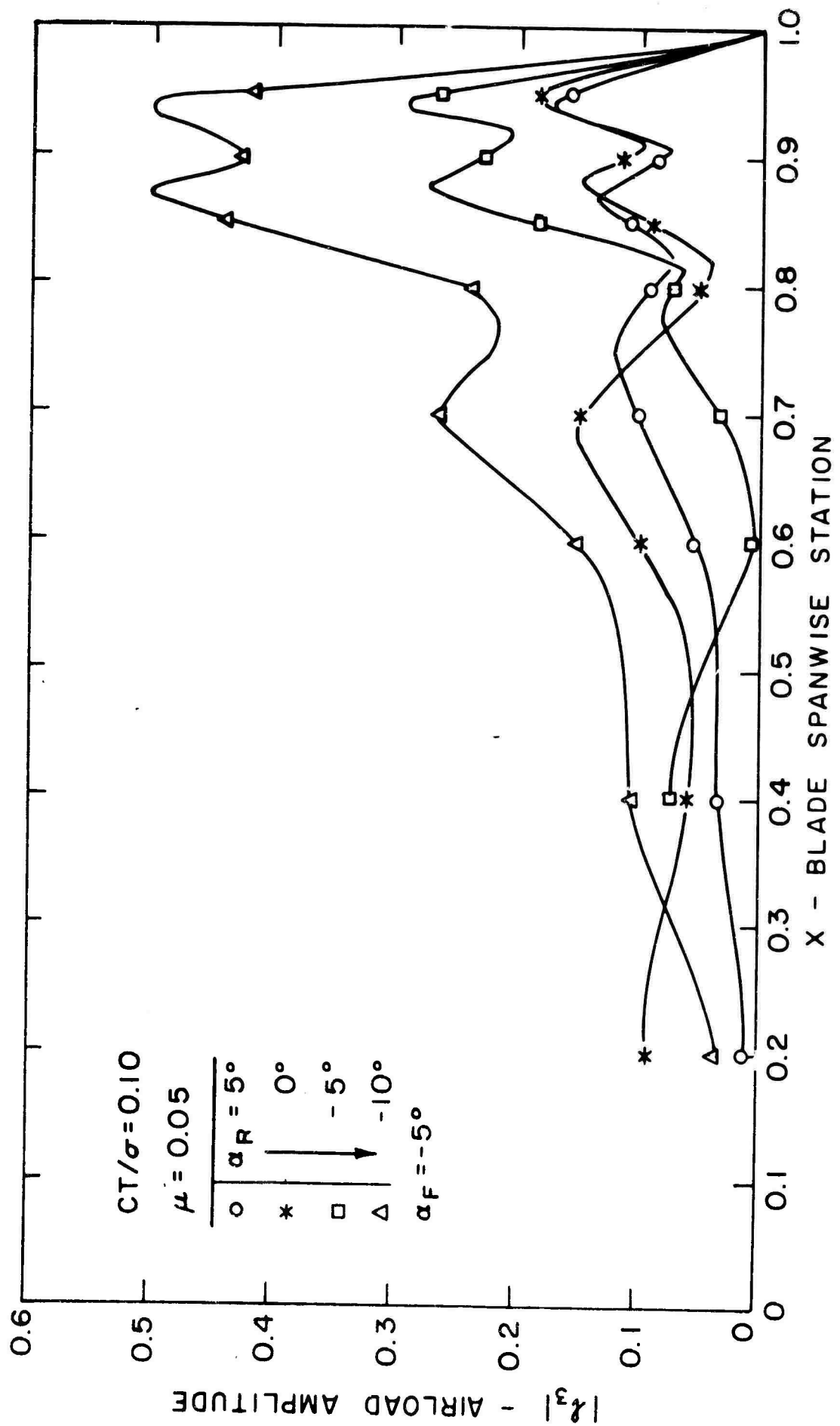


FIGURE 7(a). NONDIMENSIONAL THIRD HARMONIC AIRLOAD AMPLITUDES FOR THE REAR TANDEM ROTOR WITH RIGID BLADES.

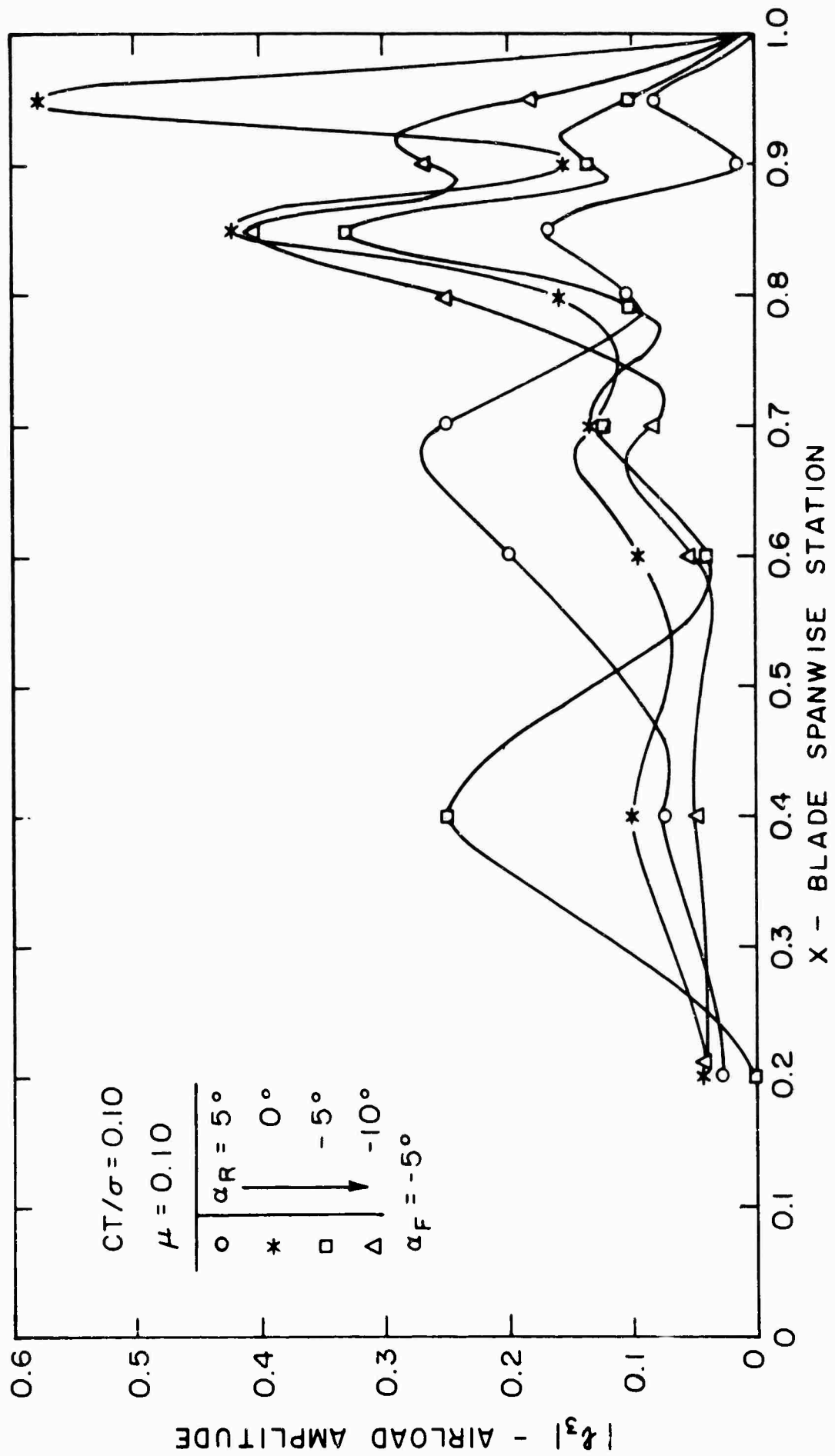


FIGURE 7(b).

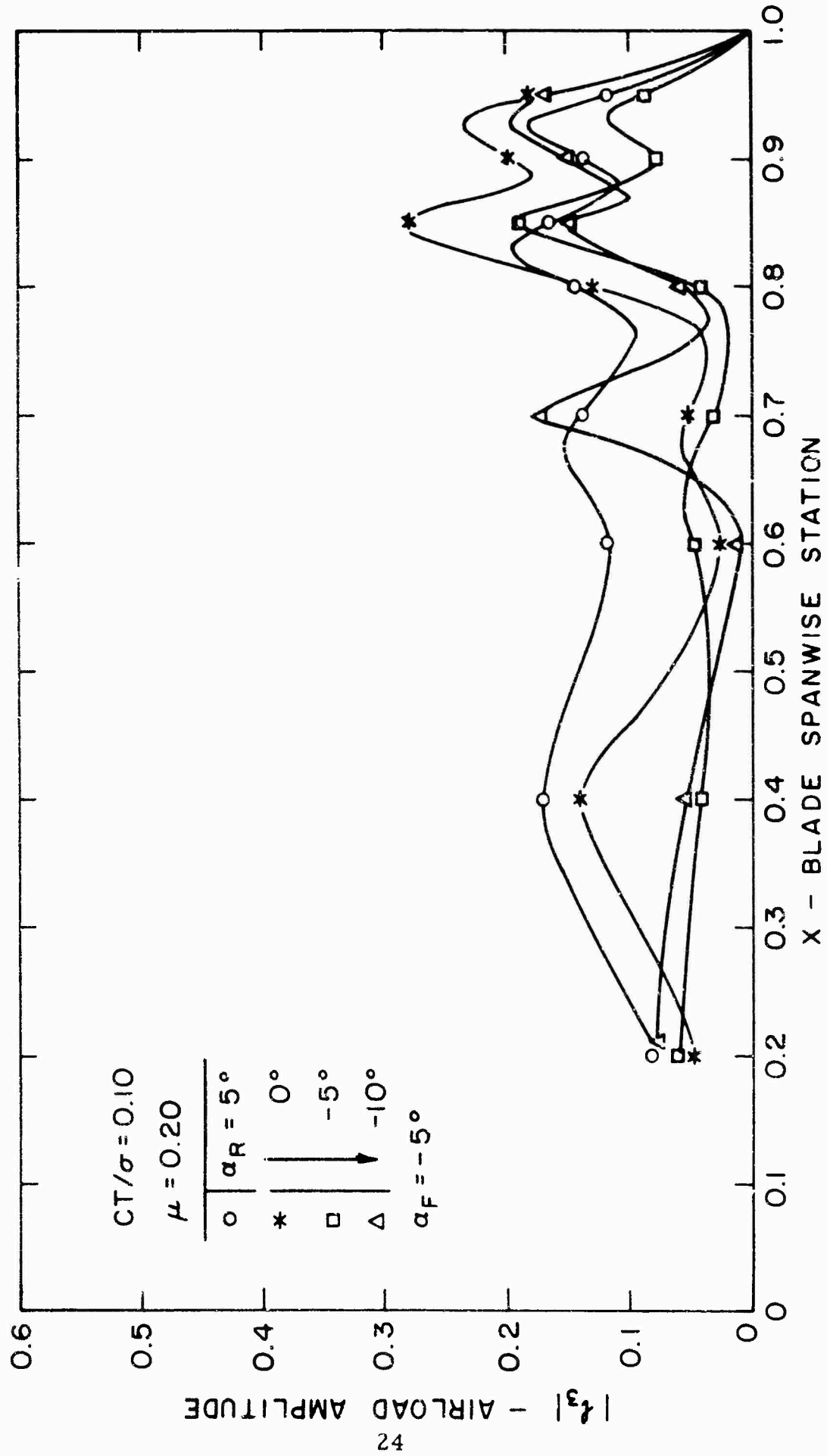


FIGURE 7(c)

$|f_3|$ - AIRLOAD AMPLITUDE

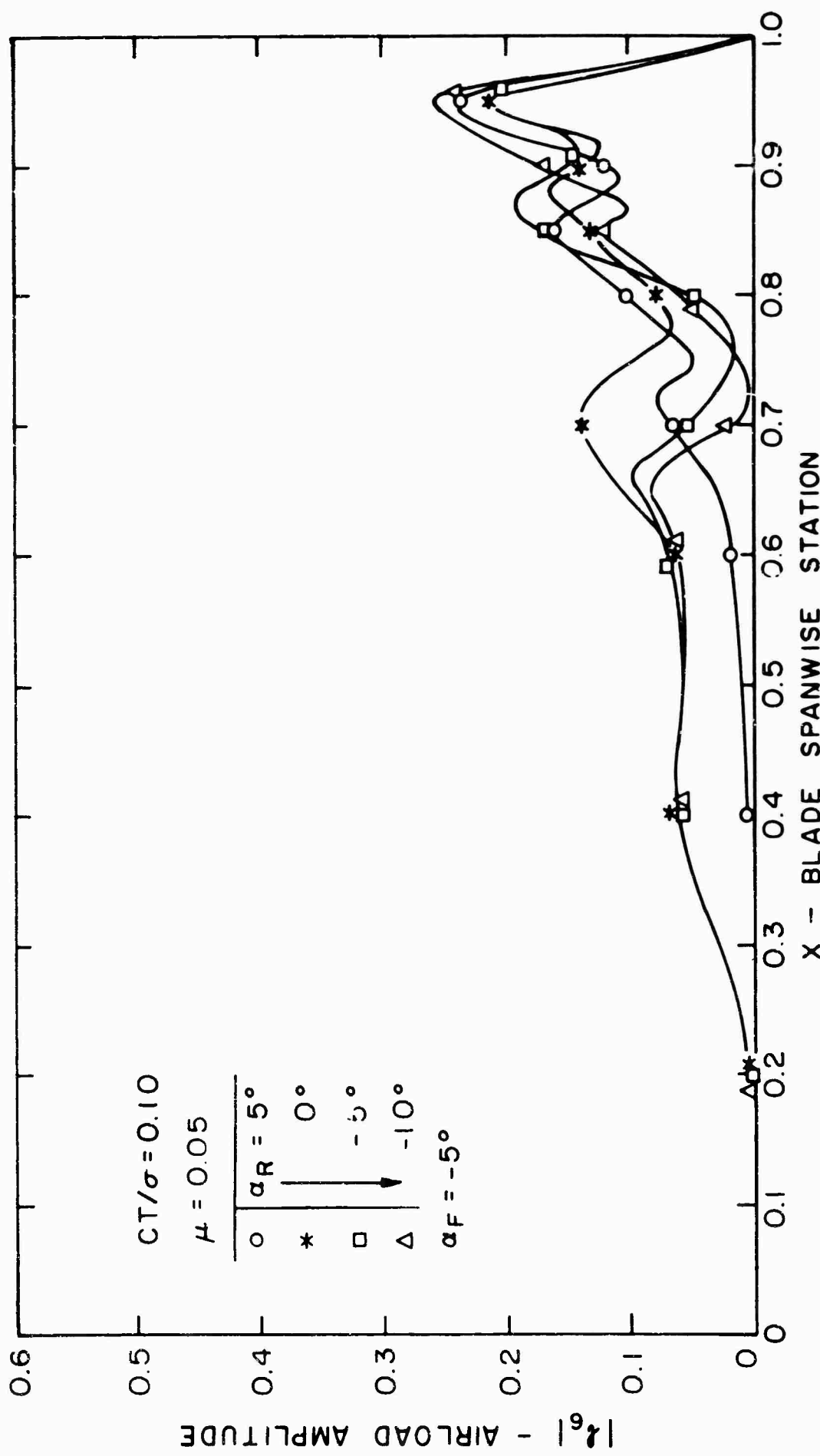


FIGURE 8(a) NONDIMENSIONAL SIXTH HARMONIC AIRLOAD AMPLITUDES FOR THE REAR TANDEM ROTOR WITH RIGID BLADES.

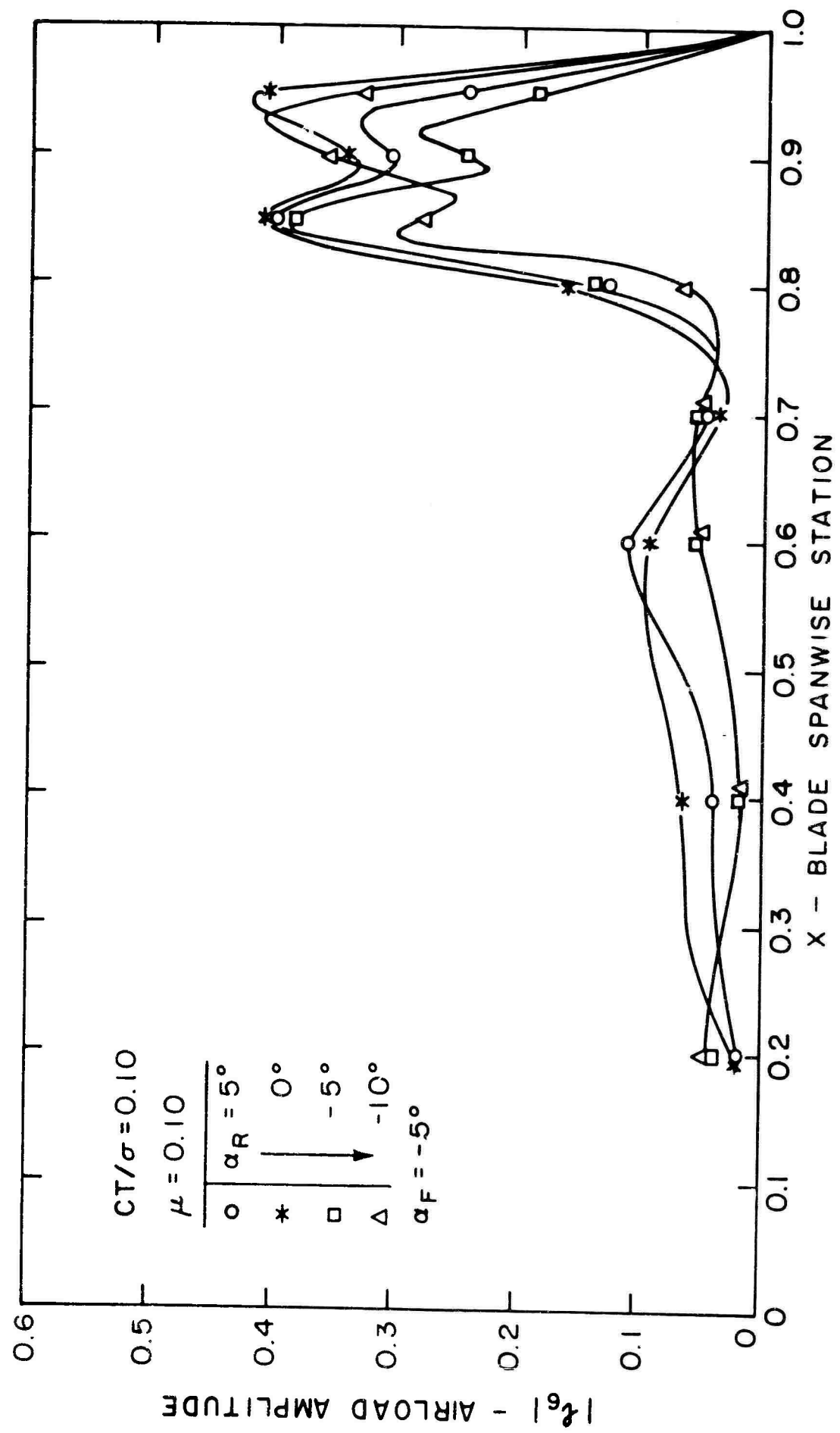


FIGURE 8(b).

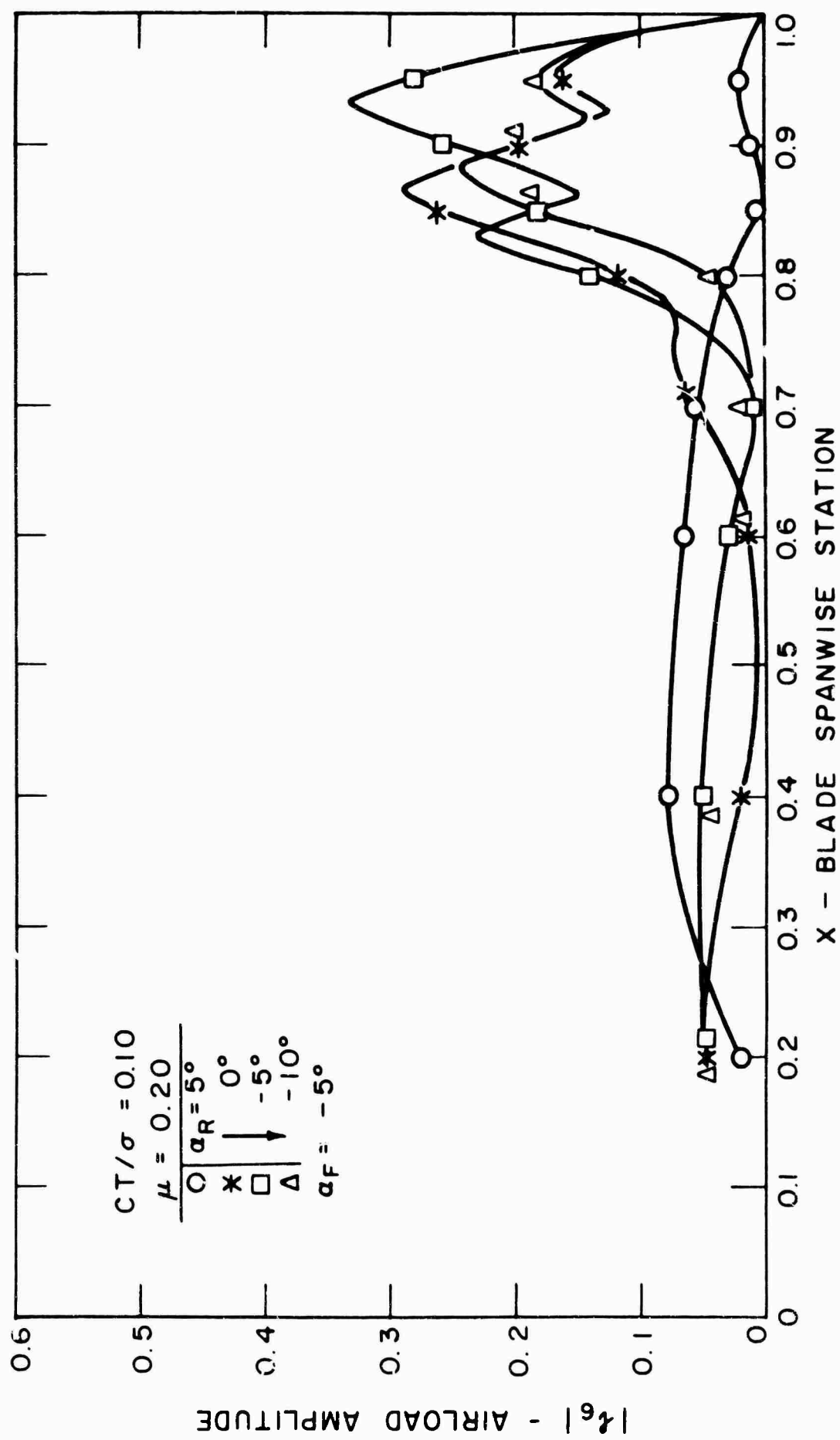


FIGURE 8(c).

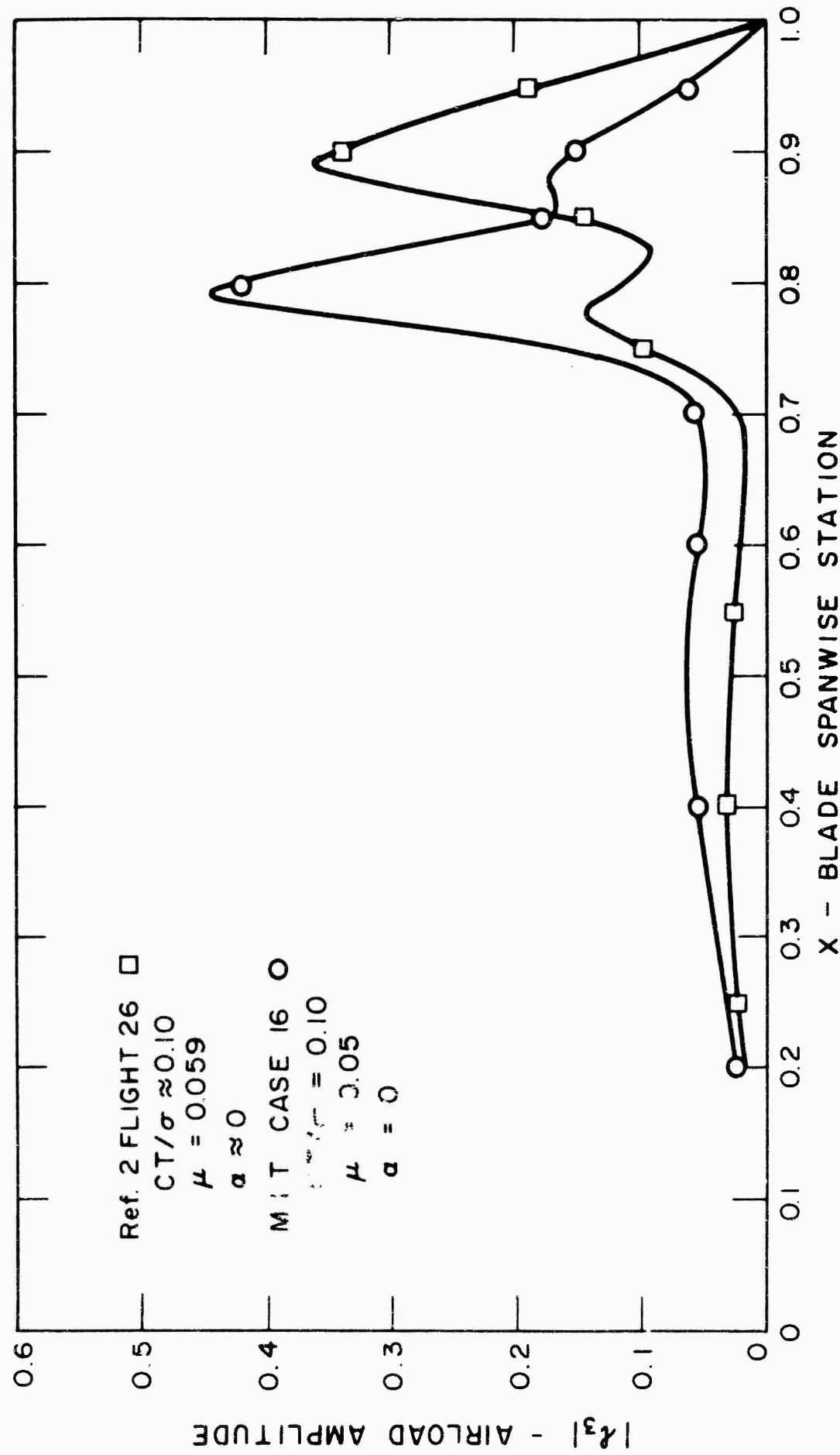


FIGURE 9(a) NONDIMENSIONAL THIRD HARMONIC AIRLOAD AMPLITUDE COMPARISON – THREE- AND FOUR-BLADED ROTORS.

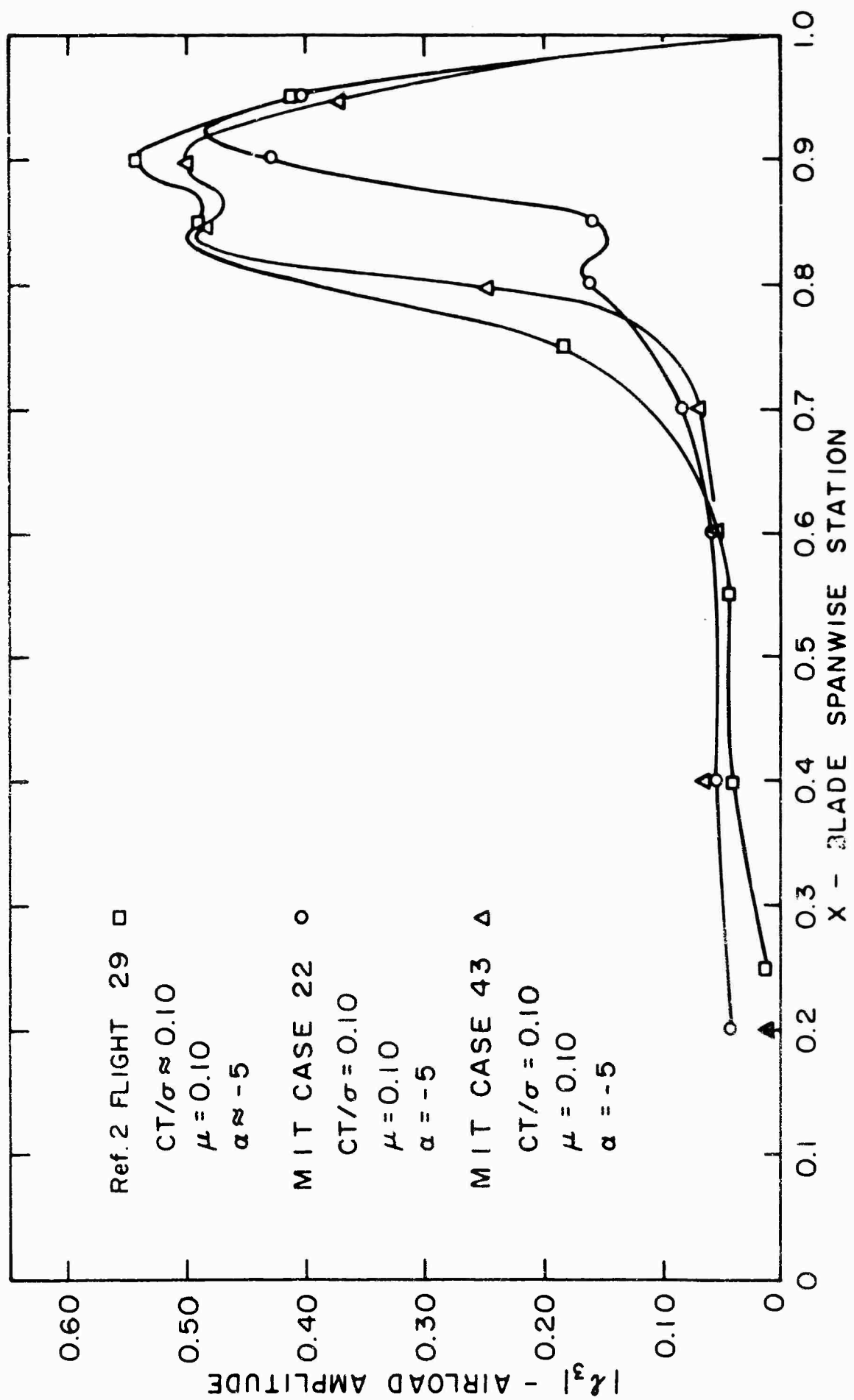


FIGURE 9 (b).

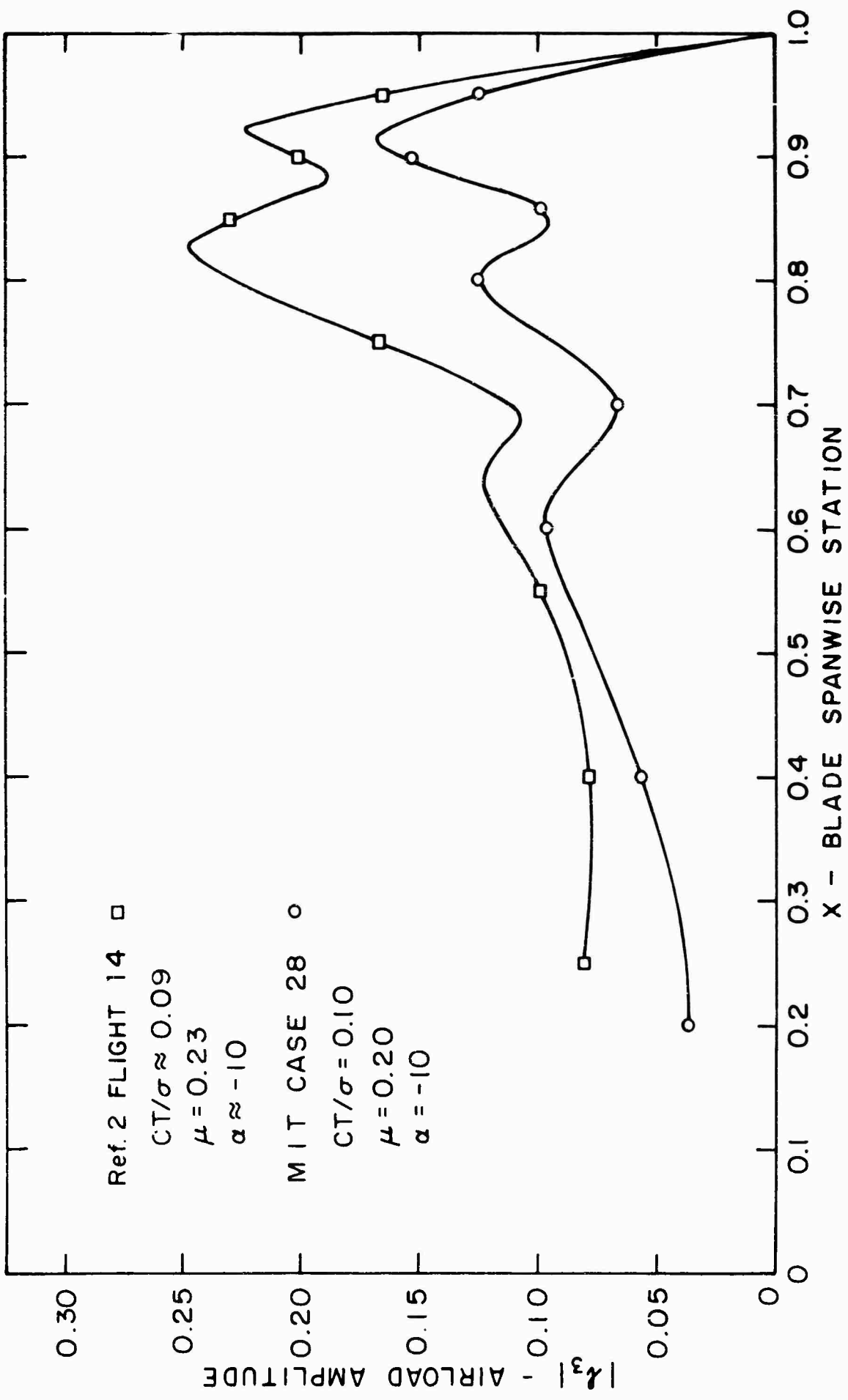
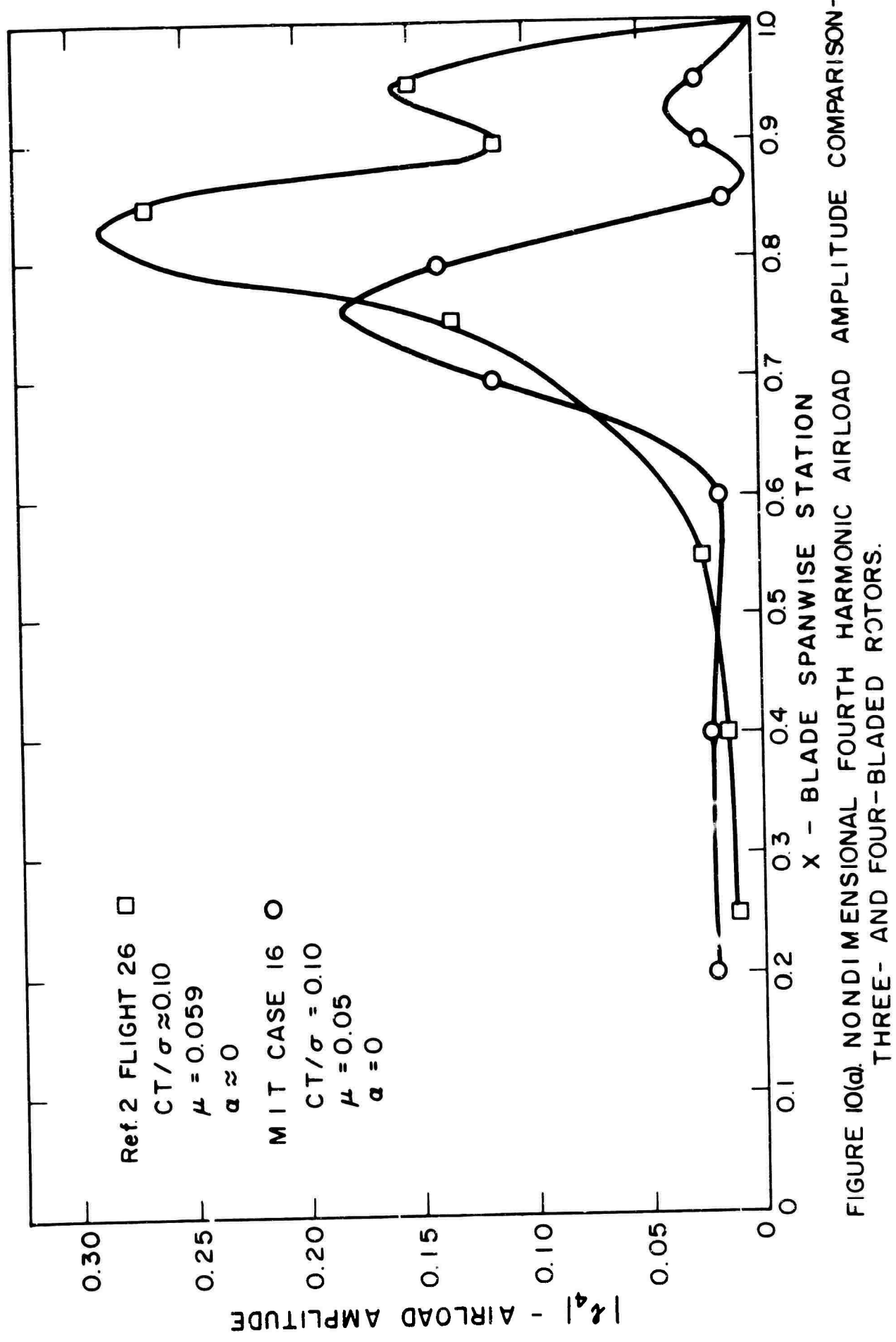


FIGURE 9(c).



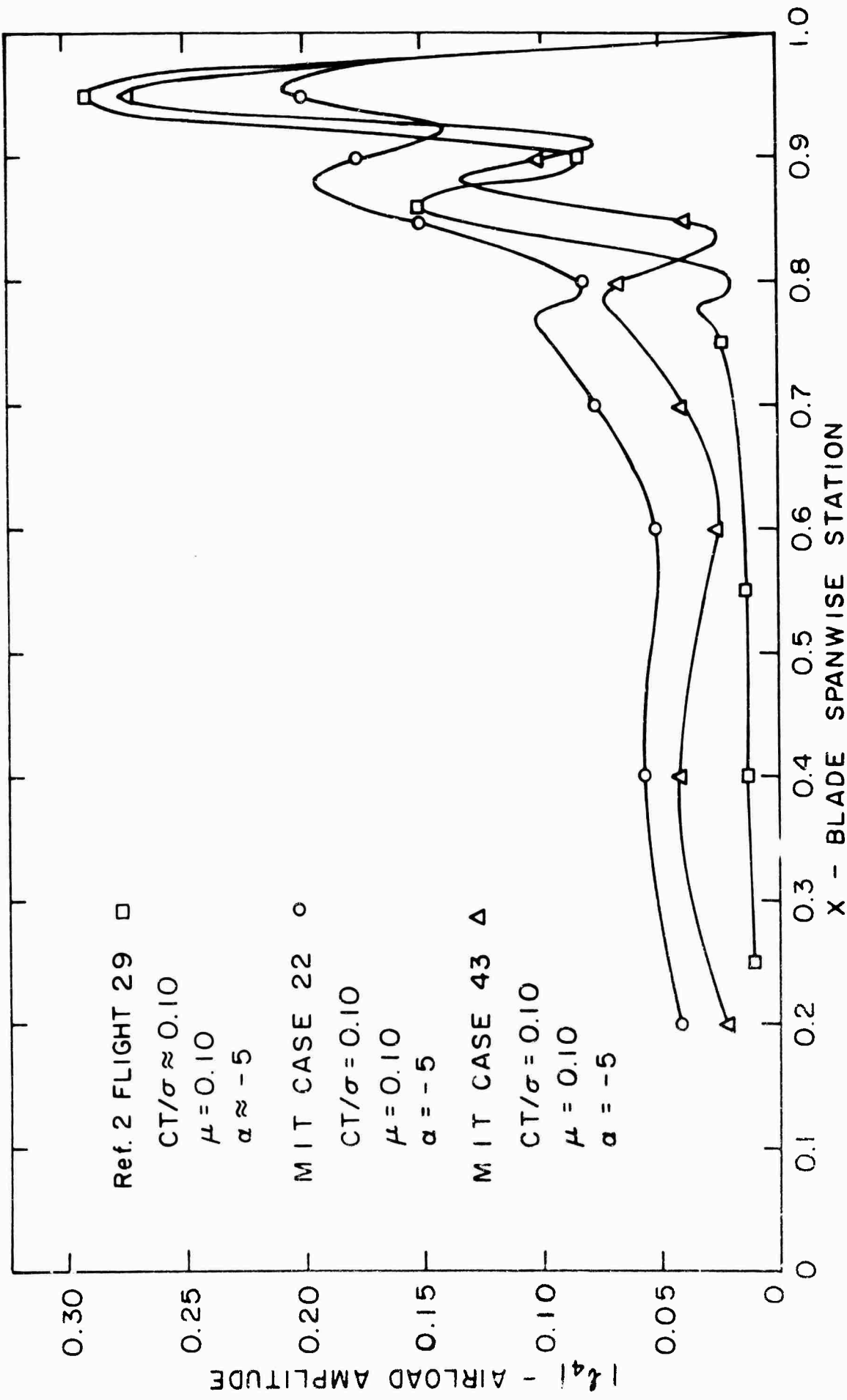


FIGURE 10 (b).

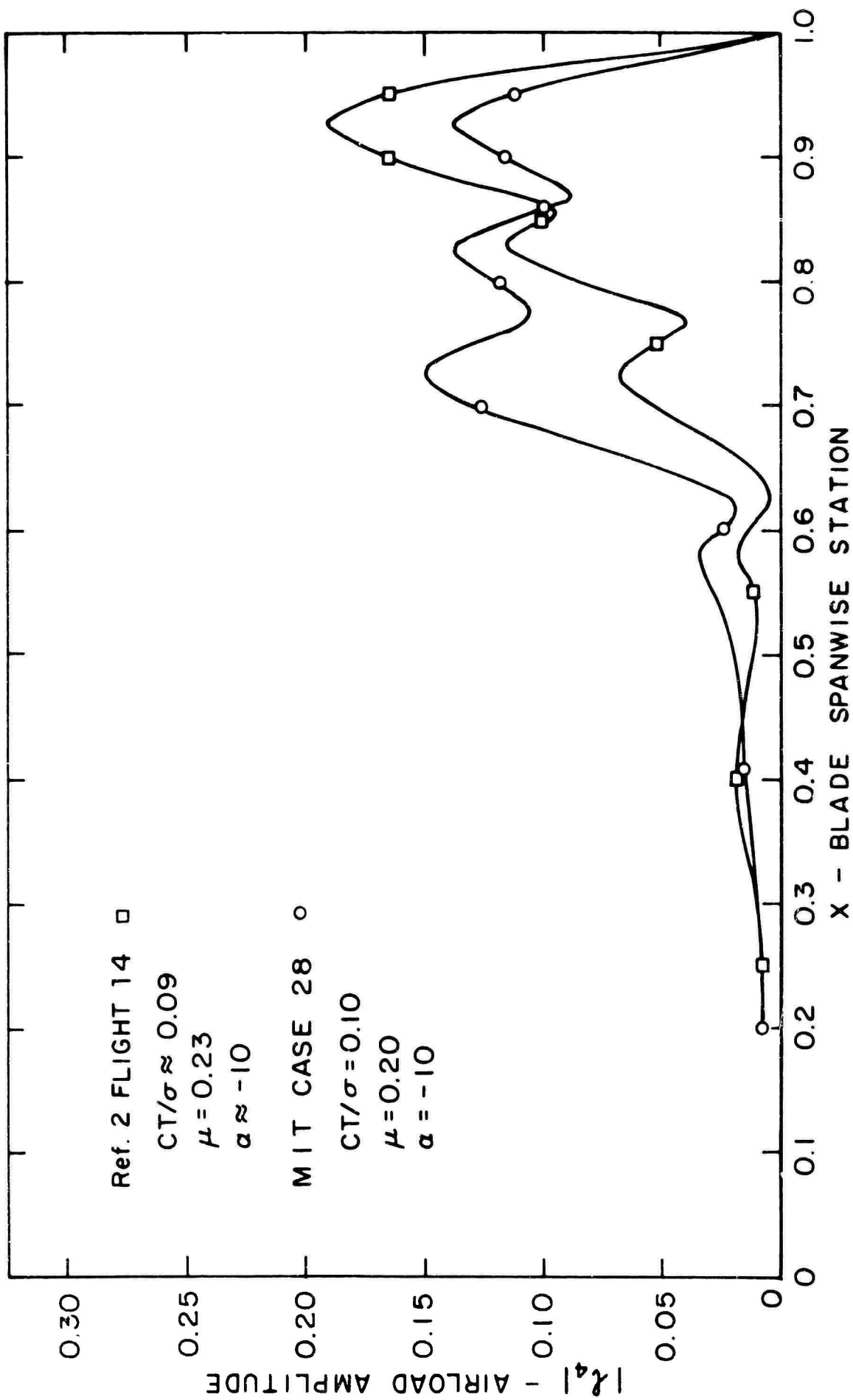


FIGURE 10(c).

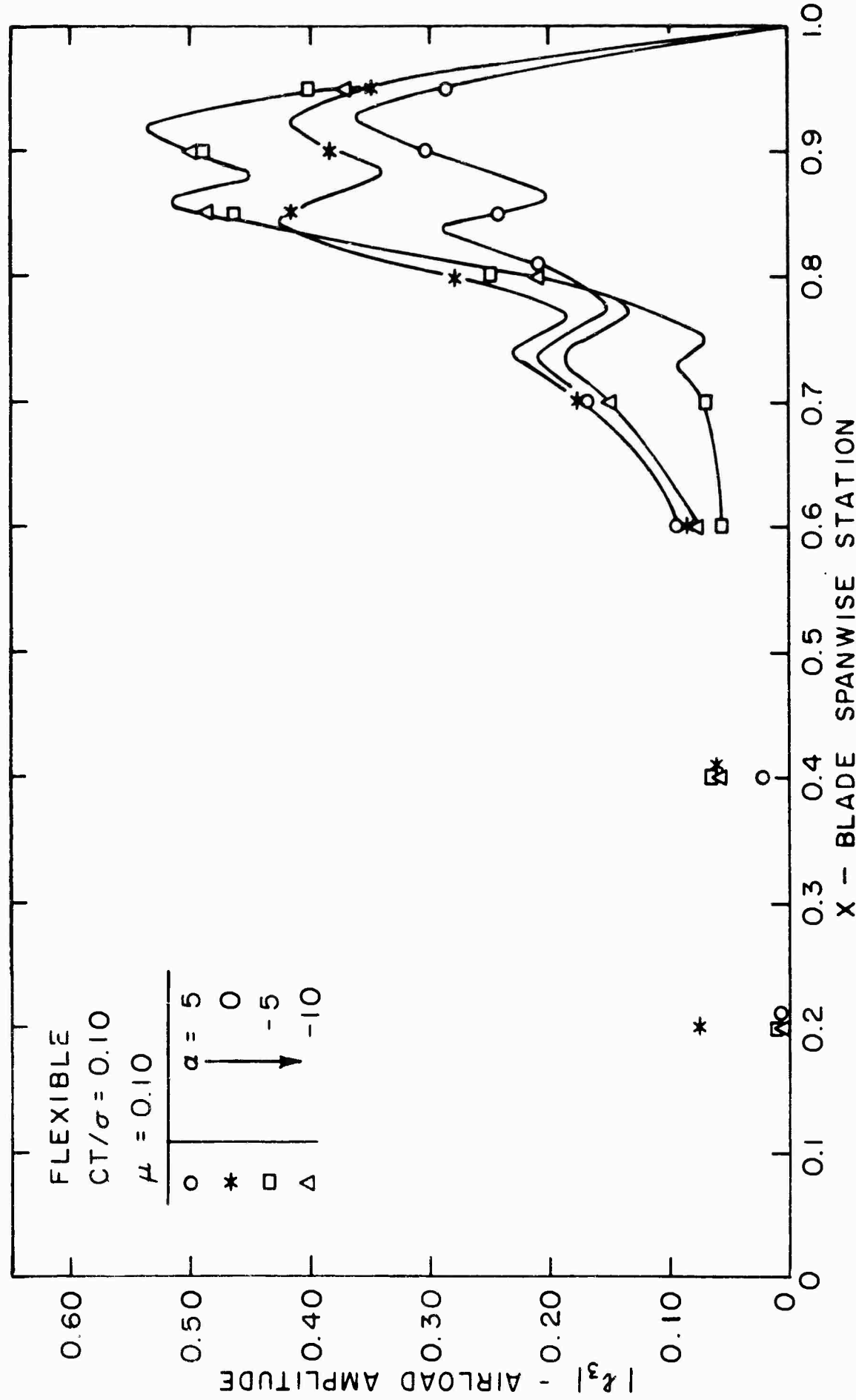


FIGURE 11. NONDIMENSIONAL THIRD HARMONIC AIRLOAD AMPLITUDES FOR THE
 SINGLE ROTOR WITH FLEXIBLE BLADES IN BENDING RESONANCE.

REFERENCES

1. Bell Helicopter Co., Measurement of Dynamic Airloads on a Full-Scale Semirigid Rotor, TCREC Technical Report TR 62-42, U.S. Army Transportation Research Command, Fort Eustis, Virginia.
2. Scheiman, J., A Tabulation of Helicopter Rotor-Blade Differential Pressures, Stresses, and Motions as Measured in Flight, NASA Technical Memorandum X-952, March 1964.
3. Miller, R.H., "Unsteady Air Loads on Helicopter Rotor Blades", Journal of the Royal Aeronautical Society, April 1964.
4. Ham, N.D., An Experimental Investigation of the Effect of a Nonrigid Wake on Rotor Blade Airloads in Transition Flight, Cornell Aeronautical Laboratory/TRC Symposium on Dynamic Load Problems Associated with Helicopters and V/STOL Aircraft, Proceedings, Vol. I., June 1963.
5. Miller, R.H., A Discussion of Rotor Blade Harmonic Airloading, same source as Ref. 4.
6. Zvara, J. and Ham, N.D., "Helicopter Rotor Model Research at M.I.T.", Journal of the American Helicopter Society, January 1960.
7. Patterson, J.L., A Miniature Electrical Pressure Gage Utilizing a Stretched Flat Diaphragm, NACA Technical Note 2659, April 1952.
8. Duvivier, J.F., Study of Helicopter Rotor-Rotor Interference Effects on Hub Vibration, Air Force Systems Command Technical Documentary Report ASD-TR-61-601, June 1962.
9. Daigle, L.L., Evaluation of Variable Reluctance Pressure Pickups for Application to Helicopter Rotor Test Rig, Report M-11554-1, United Aircraft Corp., Hartford, Connecticut, February 1954.

DISTRIBUTION

US Army Materiel Command	2
US Army Mobility Command	2
US Army Aviation Materiel Command	5
Chief of R&D, DA	1
US Army Transportation Research Command	38
USATRECOM Liaison Officer, US Army R&D Group (Europe)	1
US Army Engineer R&D Laboratories	2
Army Research Office-Durham	2
US Army Research Support Group	1
US Army Aviation School	1
US Army Aviation Test Activity	1
US Army General Equipment Test Activity	1
Air Force Systems Command, Wright-Patterson AFB	3
Air Force Flight Test Center, Edwards AFB	1
Air Proving Ground Center, Eglin AFB	1
Bureau of Naval Weapons	3
US Naval Postgraduate School	1
US Naval Air Station, Patuxent River	1
David Taylor Model Basin	1
Marine Corps Liaison Officer, US Army Transportation School	1
Ames Research Center, NASA	1
NASA Representative, Scientific and Technical Information Facility	2
National Aviation Facilities Experimental Center	1
Canadian Liaison Officer, US Army Transportation School	1
Defense Documentation Center	20
US Government Printing Office	1
Air University Library, Maxwell AFB	1
NASA-LRC, Langley Station	1

APPENDIX I
ROTOR CHARACTERISTICS

	<u>Single Rotor</u>		<u>Tandem Rotor</u>	
	Rigid	Flexible	Front	Rear
Number of blades	3	3	3	3
Rotor solidity	0.10	0.10	0.10	0.10
Rotor radius, feet	4.00	4.00	4.00	4.00
Blade chord, inches	5.00	5.00	5.00	5.00
Airfoil section	0012	0012	0012	0012
Flapping hinge offset, percent radius	2.60	2.60	2.60	2.60
Lagging hinge offset, percent radius	3.70	3.70	3.70	3.70
Linear twist, degrees	-10	-10	0	-10
Blade mass constant	8.40	7.00	8.40	8.40
Blade mass, slugs per foot	.0128	.0168	.0128	.0128
Blade c.g., percent chord	25	25	25	25
First mode bending frequency, cycles per minute, at:				
400 rpm	2000	1180	2000	2000
300 rpm	1880	960	1880	1880
Rotor hub spacing, feet, vertically	--		0	
horizontally	--		5.33	
Rotor operating rpm at $\mu = .05, .10$	400	400	400	400
$\mu = .20$	300	300	300	300

APPENDIX II
TEST CONDITIONS

Case	$(C_T/\sigma)_{nom}$	μ	α^o	θ^o	$L_o^{-1b.}$	Type
1	.05	.05	5	6.8	7.2	SR(R)
2			0	6.8	6.8	
3			-5	6.5	6.2	
4			-10	6.5	6.0	
5			-15	6.8	6.0	
6	.10	5	4.8	5.9		
7		0	4.8	5.2		
8		-5	6.5	6.4		
9		-10	6.5	5.7		
10		-15	6.8	5.3		
11	.20	5	2.6	3.2		
12		0	4.0	3.2		
13		-5	5.4	3.2		
14		-10	6.8	3.2		
15	.10	.05	5	11.6	12.5	
16			0	11.6	12.1	
17			-5	11.4	11.6	
18			-10	11.4	11.3	
19			-15	11.6	11.2	
20	.10	5	10.0	12.0		
21		0	10.0	11.3		
22		-5	11.4	12.2		
23		-10	11.4	11.5		
24		-15	11.6	11.0		
25	.20	5	7.3	6.9		
26		0	7.3	5.8		
27		-5	10.0	6.8		
28		-10	10.0	5.7		SR(R)

<u>Case</u>	<u>$(C_T/\sigma)_{nom}$</u>	<u>μ</u>	<u>a_F</u>	<u>θ_F</u>	<u>L_{oF}</u>	<u>a_R</u>	<u>θ_R</u>	<u>L_{oR}</u>	<u>Type</u>
29	.10	.05	-5	11.7	11.9	5	12.5	9.6	TRR(R)
30				11.7	11.9	0	12.5	9.3	
31				11.7	11.9	-5	12.5	9.0	
32			↓	11.7	11.9	-10	12.5	8.7	
33		.10		10.6	11.3	5	11.0	8.7	
34				10.6	11.3	0	11.0	8.0	
35				10.6	11.3	-5	12.3	8.9	
36			↓	10.6	11.3	-10	12.3	8.1	
37		.20		9.4	6.3	5	8.0	6.4	
38				9.4	6.3	0	9.3	6.2	
39				9.4	6.3	-5	10.7	6.3	
40			↓	9.4	6.3	-10	12.0	6.3	↓
41	.10	.10				5	10.0	12.0	SR(F)
42						0	10.0	11.3	
43						-5	11.4	12.2	
44						-10	11.4	11.5	↓

APPENDIX III

TEST RESULTS

CRYSTAL LIQUID											
CRYSTAL LIQUID * - 100 ALPHAS = -10 MU = -10 TAU = -11.4						CRYSTAL LIQUID * - 100 ALPHAS = -10 MU = -10 TAU = -11.4					
CASE 21		CRYSTAL LIQUID		CRYSTAL LIQUID		CASE 22		CRYSTAL LIQUID		CRYSTAL LIQUID	
STATION	-20	-40	-60	-80	-100	STATION	-20	-40	-60	-80	-100
N	LWC	LWS	LNC	LWS	LNC	N	LWC	LWS	LNC	LWS	LNC
1	-0.051335	-0.019292	-0.011770	-0.012105	-0.015568	-0.018169	-0.028055	-0.028552	-0.019494	-0.019376	-0.013546
2	-0.048164	-0.019478	-0.012823	-0.012154	-0.018500	-0.028024	-0.028075	-0.011134	-0.011131	-0.018921	-0.013670
3	-0.019624	-0.004427	-0.035927	-0.032234	-0.050536	-0.028081	-0.028111	-0.011103	-0.004185	-0.011687	-0.019780
4	-0.011132	-0.006189	-0.032825	-0.041936	-0.050512	-0.028022	-0.028115	-0.004135	-0.004134	-0.013284	-0.013276
5	-0.027198	-0.002719	-0.036360	-0.036360	-0.036360	-0.028046	-0.028053	-0.004135	-0.0015028	-0.026264	-0.025962
6	-0.022229	-0.004492	-0.002704	-0.002746	-0.001164	-0.001766	-0.001101	-0.001101	-0.006121	-0.006121	-0.006121
7	-0.004743	-0.001141	-0.004612	-0.004612	-0.001141	-0.001701	-0.001141	-0.002613	-0.004694	-0.002646	-0.002646
8	-0.006866	-0.005123	-0.005123	-0.005123	-0.005123	-0.001431	-0.001431	-0.001128	-0.000596	-0.001227	-0.001227
9	-0.015251	-0.009800	-0.002456	-0.002456	-0.001141	-0.001740	-0.001141	-0.002254	-0.000596	-0.001701	-0.001701
10	-0.027827	-0.035637	-0.002741	-0.002741	-0.001228	-0.001743	-0.001228	-0.002339	-0.001684	-0.001684	-0.001684
N	LWC	LWS	LNC	LWS	LNC	N	LWC	LWS	LNC	LWS	LNC
1	-0.128354	-0.191911	-0.003166	-0.040033	-0.011548	-0.018089	-0.000821	-0.050190	-0.010103	-0.010103	-0.011645
2	-0.041695	-0.010312	-0.034101	-0.016112	-0.018081	-0.018081	-0.000801	-0.019151	-0.010103	-0.010103	-0.011645
3	-0.053940	-0.004050	-0.075157	-0.016114	-0.060401	-0.018081	-0.002007	-0.000806	-0.010103	-0.010103	-0.011645
4	-0.039584	-0.005194	-0.028790	-0.006783	-0.018081	-0.018081	-0.003064	-0.001656	-0.010103	-0.010103	-0.011645
5	-0.034905	-0.001711	-0.026170	-0.016112	-0.018081	-0.018081	-0.001786	-0.001656	-0.010103	-0.010103	-0.011645
6	-0.007749	-0.010787	-0.018611	-0.003021	-0.018081	-0.018081	-0.002310	-0.001656	-0.004671	-0.001984	-0.001984
7	-0.002189	-0.001082	-0.002615	-0.002615	-0.001863	-0.002615	-0.002615	-0.001656	-0.004671	-0.001984	-0.001984
8	-0.005584	-0.004450	-0.017988	-0.002647	-0.018081	-0.018081	-0.001984	-0.001656	-0.004671	-0.001984	-0.001984
9	-0.023690	-0.004154	-0.001741	-0.001741	-0.001863	-0.002647	-0.001984	-0.001656	-0.004671	-0.001984	-0.001984
10	-0.0055531	-0.001986	-0.006115	-0.013114	-0.001741	-0.006102	-0.003491	-0.006102	-0.0006131	-0.0006131	-0.001045
N	LWC	LWS	LNC	LWS	LNC	N	LWC	LWS	LNC	LWS	LNC
1	-0.026252	-0.013149	-0.011506	-0.011506	-0.017846	-0.017846	-0.027605	-0.028055	-0.012497	-0.012497	-0.011645
2	-0.013917	-0.006117	-0.015159	-0.015159	-0.017846	-0.017846	-0.007072	-0.016660	-0.012497	-0.012497	-0.011645
3	-0.016887	-0.012212	-0.011100	-0.011100	-0.017846	-0.017846	-0.001042	-0.016660	-0.012497	-0.012497	-0.011645
4	-0.009560	-0.004043	-0.009463	-0.009463	-0.017846	-0.017846	-0.001656	-0.016660	-0.012497	-0.012497	-0.011645
5	-0.006560	-0.010101	-0.010101	-0.010101	-0.017846	-0.017846	-0.001656	-0.016660	-0.012497	-0.012497	-0.011645
6	-0.002615	-0.006881	-0.006881	-0.006881	-0.017846	-0.017846	-0.001656	-0.016660	-0.012497	-0.012497	-0.011645
7	-0.005584	-0.004450	-0.017988	-0.002647	-0.017846	-0.017846	-0.001783	-0.001656	-0.003491	-0.001984	-0.001984
8	-0.0023690	-0.004154	-0.001741	-0.001741	-0.001863	-0.002647	-0.001984	-0.001656	-0.003491	-0.001984	-0.001984
9	-0.0055531	-0.001986	-0.006115	-0.013114	-0.001741	-0.006102	-0.003491	-0.006102	-0.0006131	-0.0006131	-0.001045
N	LWC	LWS	LNC	LWS	LNC	N	LWC	LWS	LNC	LWS	LNC
1	-0.022258	-0.022107	-0.022107	-0.022107	-0.022107	-0.022107	-0.022121	-0.022121	-0.015120	-0.015120	-0.013546
2	-0.016496	-0.013076	-0.015050	-0.015050	-0.015050	-0.015050	-0.015050	-0.015050	-0.016647	-0.016647	-0.013546
3	-0.011441	-0.014226	-0.015267	-0.015267	-0.015267	-0.015267	-0.015267	-0.015267	-0.017843	-0.017843	-0.013546
4	-0.008664	-0.005808	-0.015267	-0.015267	-0.015267	-0.015267	-0.015267	-0.015267	-0.017843	-0.017843	-0.013546
5	-0.005584	-0.004450	-0.017988	-0.002647	-0.015267	-0.015267	-0.001783	-0.001656	-0.003491	-0.001984	-0.001984
6	-0.0023690	-0.004154	-0.001741	-0.001741	-0.001863	-0.002647	-0.001984	-0.001656	-0.003491	-0.001984	-0.001984
7	-0.0055531	-0.001986	-0.006115	-0.013114	-0.001741	-0.006102	-0.003491	-0.006102	-0.0006131	-0.0006131	-0.001045
N	LWC	LWS	LNC	LWS	LNC	N	LWC	LWS	LNC	LWS	LNC
1	-0.022238	-0.022107	-0.022107	-0.022107	-0.022107	-0.022107	-0.015120	-0.015120	-0.016647	-0.016647	-0.013546
2	-0.016496	-0.013076	-0.015050	-0.015050	-0.015050	-0.015050	-0.015050	-0.015050	-0.016647	-0.016647	-0.013546
3	-0.011441	-0.014226	-0.015267	-0.015267	-0.015267	-0.015267	-0.015267	-0.015267	-0.017843	-0.017843	-0.013546
4	-0.008664	-0.005808	-0.015267	-0.015267	-0.015267	-0.015267	-0.015267	-0.015267	-0.017843	-0.017843	-0.013546
5	-0.005584	-0.004450	-0.017988	-0.002647	-0.015267	-0.015267	-0.001783	-0.001656	-0.003491	-0.001984	-0.001984
6	-0.0023690	-0.004154	-0.001741	-0.001741	-0.001863	-0.002647	-0.001984	-0.001656	-0.003491	-0.001984	-0.001984
7	-0.0055531	-0.001986	-0.006115	-0.013114	-0.001741	-0.006102	-0.003491	-0.006102	-0.0006131	-0.0006131	-0.001045
N	LWC	LWS	LNC	LWS	LNC	N	LWC	LWS	LNC	LWS	LNC
1	-0.022238	-0.022107	-0.022107	-0.022107	-0.022107	-0.022107	-0.015120	-0.015120	-0.016647	-0.016647	-0.013546
2	-0.016496	-0.013076	-0.015050	-0.015050	-0.015050	-0.015050	-0.015050	-0.015050	-0.016647	-0.016647	-0.013546
3	-0.011441	-0.014226	-0.015267	-0.015267	-0.015267	-0.015267	-0.015267	-0.015267	-0.017843	-0.017843	-0.013546
4	-0.008664	-0.005808	-0.015267	-0.015267	-0.015267	-0.015267	-0.015267	-0.015267	-0.017843	-0.017843	-0.013546
5	-0.005584	-0.004450	-0.017988	-0.002647	-0.015267	-0.015267	-0.001783	-0.001656	-0.003491	-0.001984	-0.001984
6	-0.0023690	-0.004154	-0.001741	-0.001741	-0.001863	-0.002647	-0.001984	-0.001656	-0.003491	-0.001984	-0.001984
7	-0.0055531	-0.001986	-0.006115	-0.013114	-0.001741	-0.006102	-0.003491	-0.006102	-0.0006131	-0.0006131	-0.001045
N	LWC	LWS	LNC	LWS	LNC	N	LWC	LWS	LNC	LWS	LNC
1	-0.022238	-0.022107	-0.022107	-0.022107	-0.022107	-0.022107	-0.015120	-0.015120	-0.016647	-0.016647	-0.013546
2	-0.016496	-0.013076	-0.015050	-0.015050	-0.015050	-0.015050	-0.015050	-0.015050	-0.016647	-0.016647	-0.013546
3	-0.011441	-0.014226	-0.015267	-0.015267	-0.015267	-0.015267	-0.015267	-0.015267	-0.017843	-0.017843	-0.013546
4	-0.008664	-0.005808	-0.015267	-0.015267	-0.015267	-0.015267	-0.015267	-0.015267	-0.017843	-0.017843	-0.013546
5	-0.005584	-0.004450	-0.017988	-0.002647	-0.015267	-0.015267	-0.001783	-0.001656	-0.003491	-0.001984	-0.001984
6	-0.0023690	-0.004154	-0.001741	-0.001741	-0.001863	-0.002647	-0.001984	-0.001656	-0.003491	-0.001984	-0.001984
7	-0.0055531	-0.001986	-0.006115	-0.013114	-0.001741	-0.006102	-0.003491	-0.006102	-0.0006131	-0.0006131	-0.001045
N	LWC	LWS	LNC	LWS	LNC	N	LWC	LWS	LNC	LWS	LNC
1	-0.022238	-0.022107	-0.022107	-0.022107	-0.022107	-0.022107	-0.015120	-0.015120	-0.016647	-0.016647	-0.013546
2	-0.016496	-0.013076	-0.015050	-0.015050	-0.015050	-0.015050	-0.015050	-0.015050	-0.016647	-0.016647	-0.013546
3	-0.011441	-0.014226	-0.015267	-0.015267	-0.015267	-0.015267	-0.015267	-0.015267	-0.017843	-0.017843	-0.013546
4	-0.008664	-0.005808	-0.015267	-0.015267	-0.015267	-0.015267	-0.015267	-0.015267	-0.017843	-0.017843	-0.013546
5	-0.005584	-0.004450	-0.017988	-0.002647	-0.015267	-0.015267	-0.001783	-0.001656	-0.003491	-0.001984	-0.001984
6	-0.0023690	-0.004154	-0.001741	-0.001741	-0.001863	-0.002647	-0.001984	-0.001656	-0.003491	-0.001984	-0.001984
7	-0.0055531	-0.001986	-0.006115	-0.013114	-0.001741	-0.006102	-0.003491	-0.006102	-0.0006131	-0.0006131	-0.001045
N	LWC	LWS	LNC	LWS	LNC	N	LWC	LWS	LNC	LWS	LNC
1	-0.022238	-0.022107	-0.022107	-0.022107	-0.022107	-0.022107	-0.015120	-0.015120	-0.016647	-0.016647	-0.013546
2	-0.016496	-0.013076	-0.015050	-0.015050	-0.015050	-0.015050	-0.015050	-0.015050	-0.016647	-0.016647	-0.013546
3	-0.011441	-0.014226	-0.015267	-0.015267	-0.015267	-0.015267	-0.015267	-0.015267	-0.017843	-0.017843	-0.013546
4	-0.008664	-0.005808	-0.015267	-0.015267	-0.015267	-0.015267	-0.015267	-0.015267	-0.017843	-0.017843	-0.013546
5	-0.005584	-0.004450	-0.017988	-0.002647	-0.015267	-0.015267	-0.001783	-0.001656	-0.003491	-0.001984	-0.001984
6	-0.0023690	-0.004154	-0.001741	-0.001741	-0.001863	-0.002647	-0.001984	-0.001656	-0.003491	-0.001984	-0.001984
7</											

Case 79 RIGID ROTOR												
C7/SOL101Y = -100 ALPHAS = 5 MU = .09 THETA = 12.9												
C7/SOL101Y = -100 ALPHAS = 5 MU = .09 THETA = 12.9												
STATION	-20	-40	-60	-80	-100	-120	STATION	-20	-40	-60	-80	
N	LNC	LMS	LNC	LMS	LNC	LMS	N	LNC	LMS	LNC	LMS	
1	-0.0246801	-0.0181316	-0.0277229	-0.0476724	-0.0270701	-0.0301013	1	-0.0160164	-0.027102	-0.0190808	-0.0161032	-0.007879
2	-0.0084312	-0.0192327	-0.0130505	-0.0166972	-0.0124607	-0.0178800	2	-0.0061078	-0.0241991	-0.0213194	-0.002527	-0.0169370
3	-0.0064911	-0.0048181	-0.0061493	-0.0114937	-0.0101101	-0.0190446	3	-0.0011212	-0.0241991	-0.016476	-0.005151	-0.0026066
4	-0.0002061	-0.0011046	-0.0021627	-0.0020742	-0.0018182	-0.0190446	4	-0.0282814	-0.0111177	-0.0061180	-0.0026067	-0.0116046
5	-0.0006656	-0.0046472	-0.0062167	-0.0062166	-0.0018182	-0.0190446	5	-0.0166667	-0.0111177	-0.016476	-0.0178801	-0.0117956
6	-0.0016578	-0.0016578	-0.0016578	-0.0016578	-0.0016578	-0.0190446	6	-0.0084710	-0.0111177	-0.0011160	-0.0026067	-0.0081087
7	-0.0016578	-0.0016578	-0.0016578	-0.0016578	-0.0016578	-0.0190446	7	-0.0084710	-0.0111177	-0.0011160	-0.0026067	-0.0081087
8	-0.0016578	-0.0016578	-0.0016578	-0.0016578	-0.0016578	-0.0190446	8	-0.0084710	-0.0111177	-0.0011160	-0.0026067	-0.0081087
9	-0.0016578	-0.0016578	-0.0016578	-0.0016578	-0.0016578	-0.0190446	9	-0.0084710	-0.0111177	-0.0011160	-0.0026067	-0.0081087
10	-0.0002461	-0.0001104	-0.0001104	-0.0001104	-0.0001104	-0.0001104	10	-0.0002461	-0.0001104	-0.0001104	-0.0001104	-0.0001104
N	LNC	LMS	LNC	LMS	LNC	LMS	N	LNC	LMS	LNC	LMS	
1	-0.0160164	-0.027102	-0.0190808	-0.0161032	-0.0272890	-0.0106443	1	-0.0160164	-0.0241991	-0.0161032	-0.0131377	-0.0035130
2	-0.0061078	-0.0241991	-0.016476	-0.016476	-0.0130779	-0.0120804	2	-0.0160164	-0.0161032	-0.0161032	-0.0264600	-0.0061039
3	-0.0011212	-0.0241991	-0.016476	-0.016476	-0.0120804	-0.0120804	3	-0.0211177	-0.0132770	-0.0115020	-0.0010183	-0.0064463
4	-0.0084710	-0.0241991	-0.016476	-0.016476	-0.0120804	-0.0120804	4	-0.0084710	-0.0161177	-0.0161177	-0.0268887	-0.0413660
5	-0.0084710	-0.0241991	-0.016476	-0.016476	-0.0120804	-0.0120804	5	-0.0211177	-0.0161177	-0.0161177	-0.0273141	-0.0717940
6	-0.0084710	-0.0241991	-0.016476	-0.016476	-0.0120804	-0.0120804	6	-0.0211177	-0.0161177	-0.0161177	-0.0273141	-0.0717940
7	-0.0084710	-0.0241991	-0.016476	-0.016476	-0.0120804	-0.0120804	7	-0.0211177	-0.0161177	-0.0161177	-0.0273141	-0.0717940
8	-0.0084710	-0.0241991	-0.016476	-0.016476	-0.0120804	-0.0120804	8	-0.0211177	-0.0161177	-0.0161177	-0.0273141	-0.0717940
9	-0.0084710	-0.0241991	-0.016476	-0.016476	-0.0120804	-0.0120804	9	-0.0211177	-0.0161177	-0.0161177	-0.0273141	-0.0717940
10	-0.0084710	-0.0241991	-0.016476	-0.016476	-0.0120804	-0.0120804	10	-0.0211177	-0.0161177	-0.0161177	-0.0273141	-0.0717940
STATION	-20	-40	-60	-80	-100	-120	STATION	-20	-40	-60	-80	
N	LNC	LMS	LNC	LMS	LNC	LMS	N	LNC	LMS	LNC	LMS	
1	-0.0265440	-0.0216965	-0.0181797	-0.0161176	-0.0287390	-0.0106443	1	-0.0160164	-0.0241991	-0.0161032	-0.0131377	-0.0035130
2	-0.0185550	-0.0151716	-0.0128745	-0.0114941	-0.0180738	-0.00644206	2	-0.0160164	-0.0161032	-0.0161032	-0.0224640	-0.0061039
3	-0.0184974	-0.0081158	-0.0064206	-0.0064206	-0.0130779	-0.0120804	3	-0.0211177	-0.0132770	-0.0115020	-0.0010183	-0.0064463
4	-0.0161017	-0.0219254	-0.0169301	-0.0169301	-0.0209780	-0.00644206	4	-0.0084710	-0.0161177	-0.0161177	-0.0268887	-0.0413660
5	-0.0083844	-0.0111018	-0.0167454	-0.0167454	-0.0239462	-0.0106443	5	-0.0211177	-0.0161177	-0.0161177	-0.0273141	-0.0717940
6	-0.0016578	-0.0111018	-0.0167454	-0.0167454	-0.0239462	-0.0106443	6	-0.0211177	-0.0161177	-0.0161177	-0.0273141	-0.0717940
7	-0.0016578	-0.0111018	-0.0167454	-0.0167454	-0.0239462	-0.0106443	7	-0.0211177	-0.0161177	-0.0161177	-0.0273141	-0.0717940
8	-0.0016578	-0.0111018	-0.0167454	-0.0167454	-0.0239462	-0.0106443	8	-0.0211177	-0.0161177	-0.0161177	-0.0273141	-0.0717940
9	-0.0016578	-0.0111018	-0.0167454	-0.0167454	-0.0239462	-0.0106443	9	-0.0211177	-0.0161177	-0.0161177	-0.0273141	-0.0717940
10	-0.0002462	-0.0106452	-0.0065115	-0.0065115	-0.0065115	-0.0065115	10	-0.0002462	-0.0065115	-0.0065115	-0.0065115	-0.0065115
STATION	-20	-40	-60	-80	-100	-120	STATION	-20	-40	-60	-80	
N	LNC	LMS	LNC	LMS	LNC	LMS	N	LNC	LMS	LNC	LMS	
1	-0.0046910	-0.0104324	-0.0152117	-0.0131176	-0.0182721	-0.0106146	1	-0.0002461	-0.0106146	-0.0261000	-0.0212211	-0.0169117
2	-0.0121301	-0.0192327	-0.0222717	-0.0205960	-0.0240600	-0.0166901	2	-0.0046910	-0.0106146	-0.0218100	-0.0164612	-0.0169117
3	-0.0051211	-0.0022719	-0.0051211	-0.0051211	-0.0051211	-0.0051211	3	-0.0051211	-0.0051211	-0.0051211	-0.0122700	-0.0010183
4	-0.0022421	-0.0016454	-0.0022421	-0.0022421	-0.0022421	-0.0022421	4	-0.0022421	-0.0022421	-0.0022421	-0.0122700	-0.0010183
5	-0.0008463	-0.0022421	-0.0022421	-0.0022421	-0.0022421	-0.0022421	5	-0.0008463	-0.0022421	-0.0022421	-0.0122700	-0.0010183
6	-0.0046910	-0.0022421	-0.0022421	-0.0022421	-0.0022421	-0.0022421	6	-0.0046910	-0.0022421	-0.0022421	-0.0122700	-0.0010183
7	-0.0016578	-0.0022421	-0.0022421	-0.0022421	-0.0022421	-0.0022421	7	-0.0016578	-0.0022421	-0.0022421	-0.0122700	-0.0010183
8	-0.0016578	-0.0022421	-0.0022421	-0.0022421	-0.0022421	-0.0022421	8	-0.0016578	-0.0022421	-0.0022421	-0.0122700	-0.0010183
9	-0.0016578	-0.0022421	-0.0022421	-0.0022421	-0.0022421	-0.0022421	9	-0.0016578	-0.0022421	-0.0022421	-0.0122700	-0.0010183
10	-0.0002462	-0.0002462	-0.0002462	-0.0002462	-0.0002462	-0.0002462	10	-0.0002462	-0.0002462	-0.0002462	-0.0002462	-0.0002462
STATION	-20	-40	-60	-80	-100	-120	STATION	-20	-40	-60	-80	
N	LNC	LMS	LNC	LMS	LNC	LMS	N	LNC	LMS	LNC	LMS	
1	-0.0246801	-0.0016877	-0.0192729	-0.0160504	-0.0240626	-0.0106443	1	-0.0002461	-0.0106443	-0.0261000	-0.0212211	-0.0169117
2	-0.0246801	-0.0133595	-0.0192729	-0.0160504	-0.0240626	-0.0106443	2	-0.0046910	-0.0106443	-0.0218100	-0.0164612	-0.0169117
3	-0.0064910	-0.0012770	-0.0176492	-0.0160504	-0.0240626	-0.0106443	3	-0.0051211	-0.0106443	-0.0218100	-0.0164612	-0.0169117
4	-0.0022421	-0.0012770	-0.0176492	-0.0160504	-0.0240626	-0.0106443	4	-0.0051211	-0.0106443	-0.0218100	-0.0164612	-0.0169117
5	-0.0016578	-0.0012770	-0.0176492	-0.0160504	-0.0240626	-0.0106443	5	-0.0051211	-0.0106443	-0.0218100	-0.0164612	-0.0169117
6	-0.0016578	-0.0012770	-0.0176492	-0.0160504	-0.0240626	-0.0106443	6	-0.0051211	-0.0106443	-0.0218100	-0.0164612	-0.0169117
7	-0.0016578	-0.0012770	-0.0176492	-0.0160504	-0.0240626	-0.0106443	7	-0.0051211	-0.0106443	-0.0218100	-0.0164612	-0.0169117
8	-0.0016578	-0.0012770	-0.0176492	-0.0160504	-0.0240626	-0.0106443	8	-0.0051211	-0.0106443	-0.0218100	-0.0164612	-0.0169117
9	-0.0016578	-0.0012770	-0.0176492	-0.0160504	-0.0240626	-0.0106443	9	-0.0051211	-0.0106443	-0.0218100	-0.0164612	-0.0169117
10	-0.0002462	-0.0002462	-0.0002462	-0.0002462	-0.0002462	-0.0002462	10	-0.0002462	-0.0002462	-0.0002462	-0.0002462	-0.0002462
STATION	-20	-40	-60	-80	-100	-120	STATION	-20	-40	-60	-80	
N	LNC	LMS	LNC	LMS	LNC	LMS	N	LNC	LMS	LNC	LMS	
1	-0.0246801	-0.0016877	-0.0192729	-0.0160504	-0.0240626	-0.0106443	1	-0.0002461	-0.0106443	-0.0261000	-0.0212211	-0.0169117
2	-0.0246801	-0.0133595	-0.0192729	-0.0160504	-0.0240626	-0.0106443	2	-0.0046910	-0.0106443	-0.0218100	-0.0164612	-0.0169117
3	-0.0064910	-0.0012770	-0.0176492	-0.0160504	-0.0240626	-0.0106443	3	-0.0051211	-0.0106443	-0.0218100	-0.0164612	-0.0169117
4	-0.0022421	-0.0012770	-0.0176492	-0.0160504	-0.0240626	-0.0106443	4	-0.0051211	-0.0106443	-0.0218100	-0.0164612	-0.0169117
5	-0.0016578	-0.0012770	-0.0176492	-0.0160504	-0.0240626	-0.0106443	5	-0.0051211	-0.0106443	-0.0218100	-0.0164612	-0.0169117
6	-0.0016578	-0.0012770	-0.0176492	-0.0160504	-0.0240626	-0.0106443	6	-0.0051211	-0.0106443	-0.0218100	-0.0164612	-0.0169117
7	-0.0016578	-0.0012770	-0.0176492	-0.0160504	-0.0240626	-0.0106443	7	-0.0051211	-0.0106443	-0.0218100	-0.0164612	-0.0169117
8	-0.0016578	-0.0012770	-0.0176492	-0.0160504	-0.0240626	-0.0106443	8	-0.0051211	-0.0106443	-0.0218100	-0.0164612	-0.0169117
9	-0.0016578	-0.0012770	-0.0176492	-0.0160504	-0.0240626	-0.0106443	9	-0.0051211	-0.0106443	-0.0218100	-0.0164612	-0.0169117
10	-0.0002462	-0.0002462	-0.0002462	-0.0002462	-0.0002462	-0.0002462	10	-0.0002462	-0.0002462	-0.0002462	-0.0002462	-0.0002462
STATION	-20	-40	-60	-80	-100	-120	STATION	-20	-40	-60	-80	
N	LNC	LMS	LNC	LMS	LNC	LMS	N	LNC	LMS	LNC	LMS	
1	-0.0246801	-0.0016877	-0.0192729	-0.0160504	-0.0240626							

STATION	C/P/SOL10117 = 100.01PMA = 5 MU = +10.74E76 = 10.0		
	LNC	SNS	LMS
N	-0.0000000000000000	-0.0000000000000000	-0.0000000000000000
1	-0.0000000000000000	-0.0000000000000000	-0.0000000000000000
2	-0.0000000000000000	-0.0000000000000000	-0.0000000000000000
3	-0.0000000000000000	-0.0000000000000000	-0.0000000000000000
4	-0.0000000000000000	-0.0000000000000000	-0.0000000000000000
5	-0.0000000000000000	-0.0000000000000000	-0.0000000000000000
6	-0.0000000000000000	-0.0000000000000000	-0.0000000000000000
7	-0.0000000000000000	-0.0000000000000000	-0.0000000000000000
8	-0.0000000000000000	-0.0000000000000000	-0.0000000000000000
9	-0.0000000000000000	-0.0000000000000000	-0.0000000000000000
10	-0.0000000000000000	-0.0000000000000000	-0.0000000000000000

CASE 41
FLEXIBLE ROTOR

/ 101111 • 100 461PM • 5 May • 10 73476 • 10.0

Case 43
Platinum 60104

C750A1011Y • 100 41pm • 9 90 • 10 1pm • 11 14

100

104

	.80	.85	.90
	LWC	LMS	LNC
1	-.012383	-.0150150	-.0191020
2	.011942	.0243102	.0035411
3	.0052101	.0017314	.0013594
4	.0059697	.0006100	.0050462
5	-.0142967	-.0017401	-.0077468
6	-.0125465	-.0050501	-.0024285
7	-.0135250	-.0013346	-.0051586
8	.0134723	.000172115	.0017112
9	.0101515	-.00272115	.0013547
10	-.0043399	-.0014001	-.0003824

	LWC	LMS	LNC	LMS	LNC
1	-.004776	-.0012116	-.0014184	-.0014930	-.0014690
2	-.000494	-.0005008	-.0005008	-.0005008	-.0005008
3	-.0005703	-.0005703	-.0005703	-.0005703	-.0005703
4	-.001969	-.001969	-.001969	-.001969	-.001969
5	-.0010127	-.0010127	-.0010127	-.0010127	-.0010127
6	-.0119240	-.0119240	-.0119240	-.0119240	-.0119240
7	-.0115131	-.0115131	-.0115131	-.0115131	-.0115131
8	-.0012001	-.0012001	-.0012001	-.0012001	-.0012001
9	-.0014407	-.0014407	-.0014407	-.0014407	-.0014407
10	-.0012590	-.0012590	-.0012590	-.0012590	-.0012590

CASE 42
FLEXIBLE RODS

/ SOLIDITY = .100 ALPHA = 0.900 = 10.0

Case 44

1

10

GARRETT - BURGESS - HARRIS